Mass Spectrometry, Mechanisms, and Molecular Models - Combining Research in Mass Spectrometric Reaction Monitoring and Chemical Education

by

Natalie L. Dean
B.Sc. (Hons), University of Victoria, 2015

A Thesis Submitted in Partial Fulfillment
of the Requirements for the Degree of

MASTER OF SCIENCE

in the Department of Chemistry

Supervisory Committee

Mass Spectrometry, Mechanisms, and Molecular Models - Combining Research in Mass Spectrometric Reaction Monitoring and Chemical Education

by

Natalie L. Dean
B.Sc. (Hons), University of Victoria, 2015

Supervisory Committee

Dr. J. Scott McIndoe, Department of Chemistry
Supervisor

Dr. Lisa Rosenberg, Department of Chemistry
Departmental Member

Abstract

This thesis combines work in the areas of mass spectrometric reaction monitoring and chemical education.

In the first part of this thesis, real-time mechanistic analysis using electrospray ionization mass spectrometry is reported. In Chapter 1, an introduction to the mass spectrometric instrumentation and methodologies used in this research is provided. In Chapter 2, the real-time mechanistic analysis of the Hiyama cross-coupling reaction using electrospray ionization mass spectrometry is reported, in particular, the fluoride-mediated rearrangement of phenylfluorosilanes that was found to occur even before catalyst addition. Combining Ph_3SiF with a fluoride ion source under typical Hiyama cross-coupling conditions causes rapid formation of the expected $[Ph_3SiF_2]^-$; however, ESI-MS analysis reveals that phenyl-fluoride exchange occurs concomitantly, also producing substantial quantities of $[Ph_nSiF_{5-n}]^-$ (n = 0-2). The exchange process is verified using ^{19}F NMR spectroscopy. This observation may have implications for Hiyama reaction protocols, which use transmetallation from triaryldifluorosilicates as a key step in cross-coupling. Optimization of the methodology used for real-time analysis by ESI-MS to reduce observed contamination from leaching of rubber septa additives is also discussed.

In the second part of this thesis, the development and application of two different approaches for generating molecular models for the teaching molecular geometry and VSEPR theory in first year chemistry is reported. Chapter 4 details a method for the application of handheld 3D printing pens for producing models from ABS plastic. In Chapter 5, the development of laser-cut acrylic model kits is detailed, as well as the design and results of a quantitative study aimed at assessing their effectiveness for improving representational competence and comprehension of molecular geometry.

Table of Contents

List of Figures

List of Tables

List of Schemes

List of Abbreviations

ABS	Acrylonitrile butadiene styrene
DCM	Dichloromethane
DEPT	Distortionless Enhancement by Polarization Transfer
DMF	N,N-dimethylformamide
DMSO	Dimethyl sulfoxide
EI	Electron impact
ESI	Electrospray ionization mass spectrometry
ESI(-)-MS	Negative-ion electrospray ionization mass spectrometry
GC-MS	Gas chromatography–mass spectrometry
HMPA	Hexamethylphosphoramide
KE	Kinetic energy
LC-MS	Liquid chromatography–mass spectrometry
m/z	Mass to charge ratio
MeCN	Acetonitrile
MeOH	Methanol
MS	Mass spectrometry/ mass spectrometer/ mass spectrum
MS/MS	Tandem mass spectrometry
MWU	Mann-Whitney U
NMR	Nuclear magnetic resonance
PSI	Pressurized sample infusion
Q-TOF	Quadrupole-time-of-flight
SD	Standard deviation
TA	Teaching assistant
TASF	Tris(dimethylamino)sulfonium difluorotrimethylsilicate
TBAF	Tetrabutylammonium fluoride
THF	tetrahydrofuran
TOF	Time-of-flight
TQD	Triple Quadrupole Detector
UV-Vis	Ultraviolet–visible
VSEPR	Valence shell electron pair repulsion

Acknowledgements

Firstly, I would like to thank my supervisor, Dr. J. S. McIndoe – not only for his immense support, patience, and guidance over the past five years – but also for providing me with the opportunity to pursue ideas and research I was passionate about. I thank you for all that you have taught me, both as a researcher and a person.

I gratefully acknowledge Corrina Ewan, Dr. Chris Barr, Dr. Ori Granot, and Sean Adams for all their hard work and assistance, as well as the generous support of UVic's Learning and Teaching Center for making my research possible. I also want to thank Dr. Dave Berry and Kelli Fawkes, for mentoring me both as a student and a teacher – you have taught me so much and ignited my passion for teaching.

I would also like to thank the *many* members of the McIndoe research group that I have had the pleasure to work with over the years. A special thanks to Darien Yeung, Rhonda Stoddard, Dr. Harmen Zijlstra, and Dr. Johanne Penafiel for being such great friends and helpful co-workers.

Finally, I would like to thank Adam Paulson for being so supportive and *always* believing (I appreciate you), and my amazing parents who have always been my biggest supporters and encouragers – I truly couldn't have done it without you.

Dedication

For Mom and Dad.

‘scientia ac labore’

Part I: Real-Time Mechanistic Analysis by Electrospray Ionization Mass Spectrometry

Chapter 1. Introduction to Reaction Monitoring by Electrospray Ionization Mass Spectrometry

1.1 Mass Spectrometry

Mass spectrometry (MS) is an analytical technique that allows for the generation, separation, and detection of ions based on their mass-to-charge ratio (*m/z*). The foundation for mass spectrometry lies in pioneering work done by J. J. Thomson in 1913, who demonstrated the separation and detection of gas-phase neon isotopes in the presence of magnetic and electric fields.[1] This discovery lead to the 1919 development of the 'mass spectrograph' by F.W. Aston, who received the 1921 Nobel Prize in Chemistry for his work.[2]

1.2 Instrumentation

Mass spectrometers consist of three fundamental components (Figure 1.1): an ion source to generate gas-phase ions, a mass analyzer to separate the ions by their *m/z*, and a detector.[3]

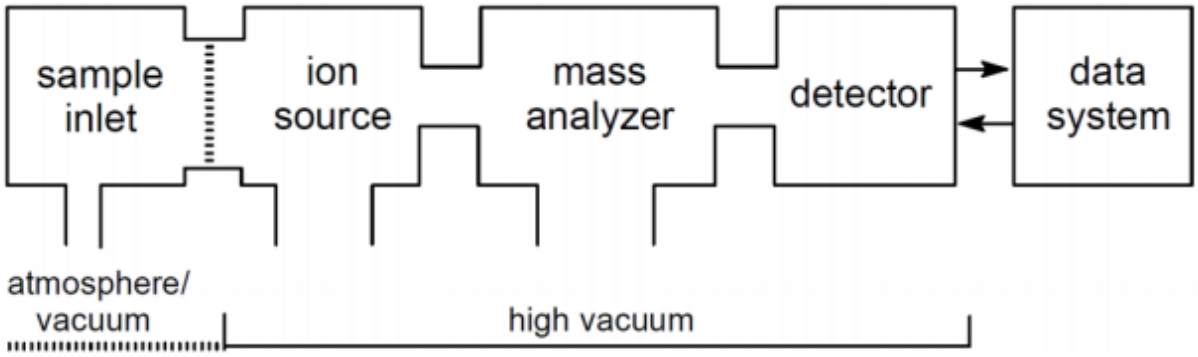

Figure 1.1 Schematic diagram of a mass spectrometer

There are many types of each component available, all with their own respective advantages and disadvantages depending on the desired application. The mass spectrometer used for this work has an electrospray ionization source and a hybrid quadrupole/time-of-flight mass analyzer, components which this chapter will describe in more detail.

1.2.1 Electrospray Ionization

Electrospray ionization mass spectrometry (ESI-MS) is a technique whereby ionic analytes are transferred from the solution phase to the gas phase via a spray of highly charged droplets.[4] It is classified as a "soft" ionization technique owing to the fact that it does not readily fragment ions, unlike "hard" ionizations methods such as electron impact. As the electrospray process does not usually impart enough energy to generate ions from neutral molecules, the analyte of interest must either be inherently charged, adventitiously charged (e.g. through protonation, cationization, etc.), or derivatized with a "charge-tagged" compound.[5] Exceptions exist only for the most electron-rich compounds, which can be oxidized to the radical cation.[6]

The electrospray ionization process involves three main steps: generation of highly charged droplets from the analyte solution, liberation of the ions from the droplets, and transport of the ions to the mass analyzer.[4,7] The analyte solution is introduced into the source via a charged stainless-steel capillary at atmospheric pressure. As a result of the strong electric field, a fine aerosol of highly charged droplets is produced as the solution passes through the capillary (Figure 1.2).

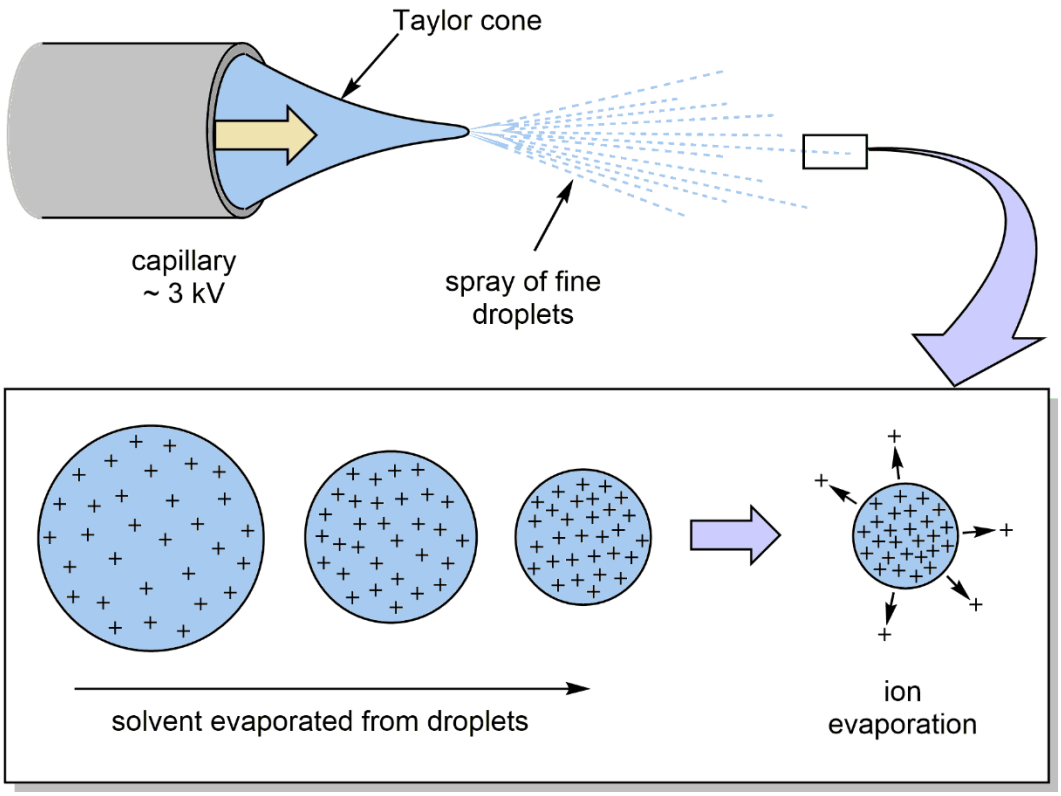

Figure 1.2 The formation of a fine spray of charged droplets by means of a charged capillary and the desolvation process in ESI-MS. [Adapted from "Mass Spectrometry of Inorganic and Organometallic Compounds: Tools-Techniques-Tips (2005)][5]

The droplets undergo rapid drying in the presence of a warm bath gas, resulting in solvent evaporation. As loss of solvent occurs, the charge density — and therefore the repulsion between the ions in the droplets— increases to the point where ions depart from the droplet. This process is thought to occur via two mechanisms: ion evaporation or Coulombic explosion; however, recent literature indicates that it is likely to occur via the ion evaporation model, at least for smaller ions.[8] The liberated ions are electrostatically drawn into the evacuated mass spectrometer and guided to the mass analyzer.

Solvent choice is important for dictating efficacy of the electrospray process and depends primarily on solubility of the analyte in the solvent, and compatibility of the solvent with the electrospray process. The solubility of the analyte is paramount as the electrospray process is not

capable of transferring undissolved solids into the gas phase, preventing analysis and even resulting in clogging of the capillary or sampling cone. In addition to solubility, the compatibility of the solvent with the electrospray ionization process is dependent on several criteria, the most prominent being volatility and polarity. As desolvation is a key step in the electrospray process, the volatility of the solvent greatly influences the efficacy of which gas phase ions are produced. Employing lower boiling point solvents also reduces the need for elevated source and desolvation temperatures, which can result in sample decomposition. Solvent polarity is also important to consider when choosing an appropriate solvent for ESI-MS, as the electrospray process is electrochemical, and therefore requires a solvent capable of providing a conductive solution.[9,10] Some commonly employed ESI-MS solvents include: water, methanol, ethanol, and acetonitrile, as a result of their moderate boiling points and polarities.[5]

1.2.2 Quadrupole Time of Flight Mass Analyzer

The hybrid Q-ToF mass analyzer is comprised of three main parts (Figure 1.3): the quadrupole analyzer (MS1), the hexapole collision cell, and the TOF (MS2).[11]

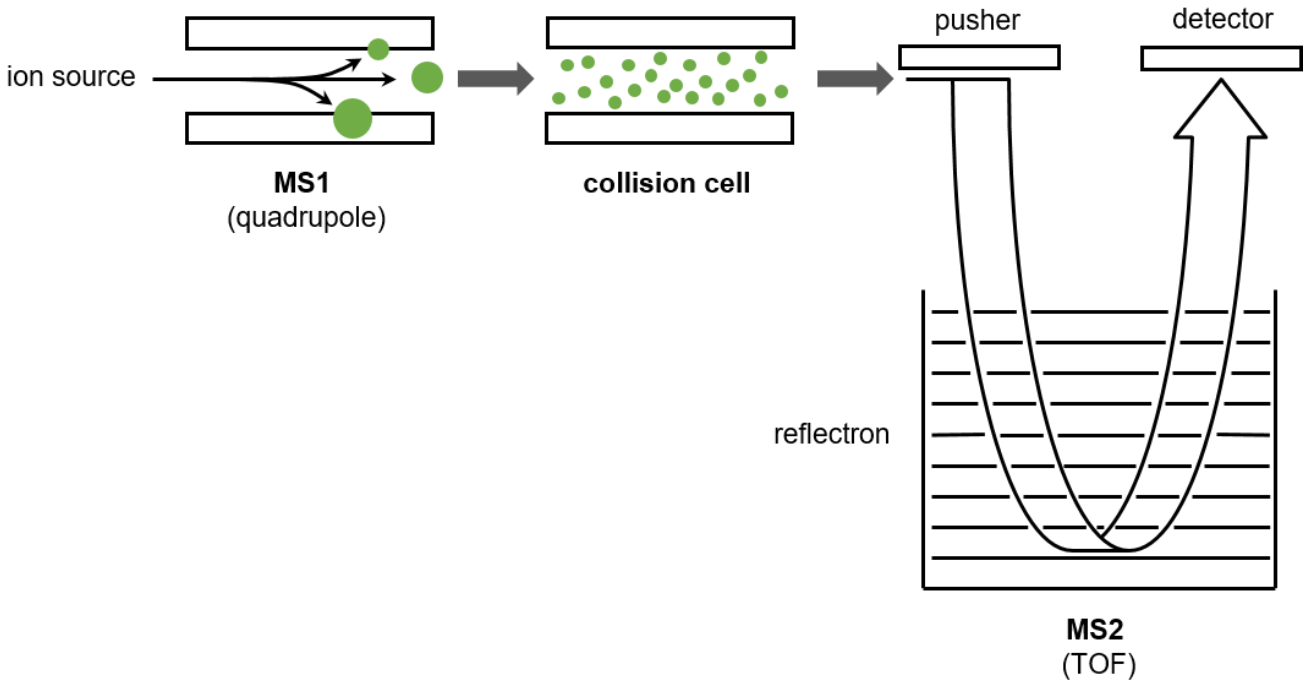

Figure 1.3 Schematic diagram of a hybrid quadrupole time of flight mass analyzer. [Adapted from "Mass Spectrometry of Inorganic and Organometallic Compounds: Tools-Techniques-Tips (2005)][5]

The quadrupole is made up of four parallel cylindrical rods, arranged as shown in Figure 1.4.[11] The quadrupole (MS1) can be set to act either as an ion guide or a mass selector, depending on the applied electric field. For typical mass spectrometric studies, the quadrupole is set to an rf-only mode which causes it to guide ions of all *m/z* values through the collision cell to the TOF (MS2).

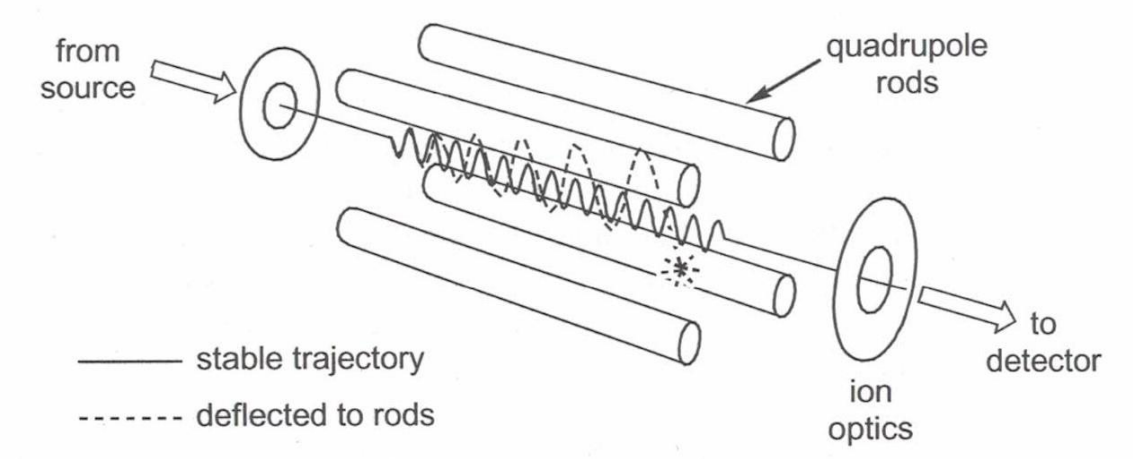

Figure 1.4 Schematic diagram of a quadrupole

For tandem-MS (MS/MS) experiments where mass selection is desired, a combination of alternating radio frequencies and static potential are applied to the rods causing ions to undergo a complex trajectory determined by their mass-to-charge ratio. Under the influence of the combined applied electric fields, only the trajectories of ions with certain mass-to-charge ratios are stabilized and passed to the collision cell, while the remainder are discharged on the poles. Once these precursor ions reach the collision cell, they are collided with gas molecules and fragmented before being passed on to MS2.

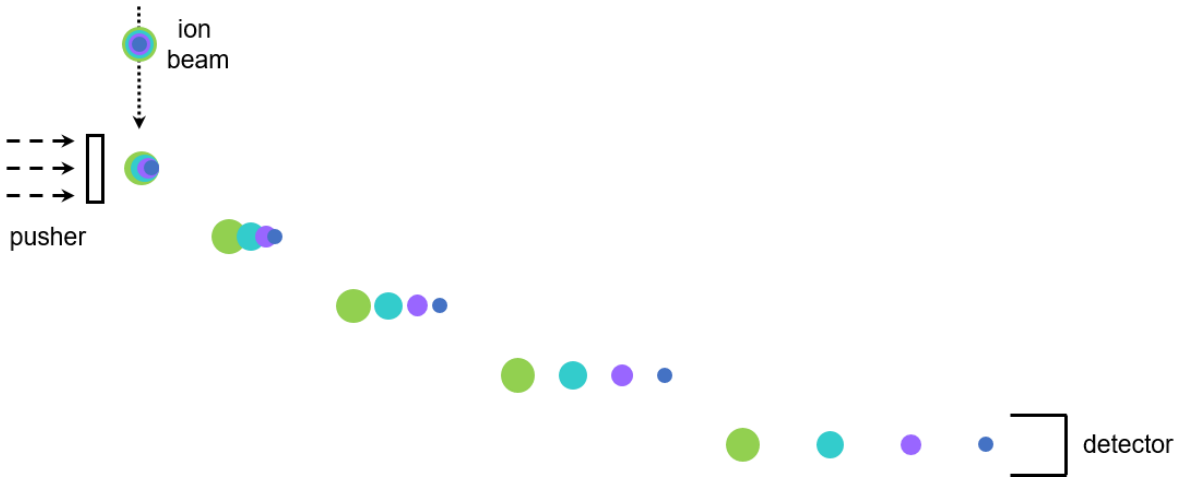

Figure 1.5 Separation of ions by a time-of-flight mass analyzer.

As the ions reach MS2, the time-of-flight mass analyzer, they are accelerated by a pulsing electrode ("pusher") into a field-free drift tube where they are separated by flight time (Figure 1.5). The pusher imparts the same amount of kinetic energy to each ion and therefore the velocity and resulting flight time of each ion is determined by its mass. Smaller ions will travel faster and reach the detector before ions with larger masses, allowing for separation of ions by *m/z*. In reality, for ions of a given *m/z*, there is a distribution of initial kinetic energies, and therefore slightly different flight times. This effect is accounted for and corrected by a reflectron (Figure 1.6), an ion mirror that reverses the flight trajectory of the ions and synchronizes their flight time. For a given *m/z*, ions which are travelling faster will penetrate further into the electric field of the ionic mirror than their slower moving counterparts. This results in synchronous arrival of the ions at the detector, which reduces the spread in flight time for ions of the same *m/z*, increasing resolution.[12]

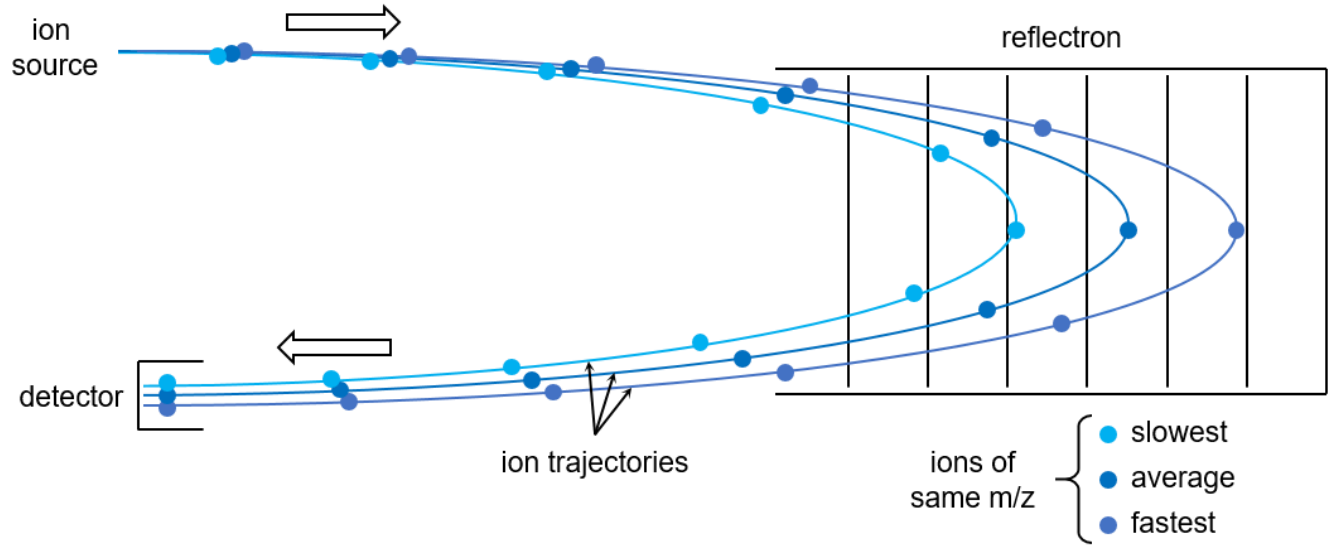

Figure 1.6 Flight trajectory of three ions of identical m/z but different kinetic energies in a time-of-flight mass analyzer with a reflectron. [Adapted from "Mass Spectrometry of Inorganic and Organometallic Compounds: Tools-Techniques-Tips (2005)][5]

1.3 Continuous Reaction Monitoring by ESI-MS

Elucidation of reaction mechanisms is complicated by the fact that most reactions include short-lived intermediates which are difficult to detect. The McIndoe research group has developed methodologies - in particular, continuous monitoring of reactions via pressurized sample infusion coupled with electrospray ionization mass spectrometry - that facilitate mechanistic studies on difficult problems.[13–15]

1.3.1 Pressurized Sample Infusion

Pressurized sample infusion (PSI) allows for real-time monitoring of a reaction by providing a continuous flow of the reaction solution to the instrument for the duration of the experiment. A slight overpressure (1-5 psi) of a gas, typically Ar or N_2, is applied to the reaction flask allowing for a cannula-type transfer of the solution into the instrument at an appropriate flow rate for mass spectrometry (Figure 1.7).

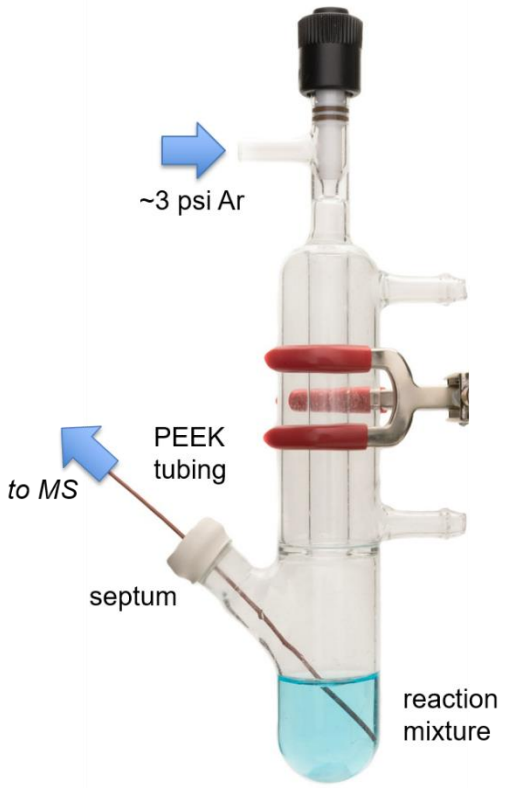

Figure 1.7 Pressurized sample infusion (PSI) allows for real-time monitoring by providing continuous infusion of a reaction solution to the mass spectrometer

1.3.2 Catalytic Reaction Monitoring

ESI-MS is well suited to the analysis of organometallic compounds and catalytic reactions and has developed into a powerful tool for mechanistic elucidation of homogeneous catalytic systems.[15] Being a soft ionization technique, ESI-MS is ideal for the analysis of low ionization-efficiency species, such as unstable catalytic intermediates, as it allows for transfer of ions into the gas-phase with minimal fragmentation. This enables real-time analysis of catalytic reactions, including observation of transient catalytic intermediates, which allows for important kinetic and mechanistic data to be obtained.

Unlike methods of analysis such as NMR or UV-Vis spectroscopy, ESI-MS is well suited to the analysis of complex mixtures. The high sensitivity and large dynamic range of this method of analysis allows for the detection of abundant and trace species alike; and the fast, one second scan time allows for highly dense data to be collected for kinetic analysis as well as detection of short-lived intermediates.[15] ESI-MS also tends to produce clean, easily interpretable spectra as a result of the low occurrence of fragmentation.

Chapter 2. Mechanistic Investigation of the Fluoride-mediated Rearrangement of Phenylfluorosilanes in the Hiyama Cross-Coupling Reaction by ESI-MS

Portions of this section are reproduced with permission from "Fluoride-mediated rearrangement of phenylfluorosilanes" N. L. Dean, J. S. McIndoe. Can. J. Chem., in press © 2018 Canadian Science Publishing.

2.1 Introduction

The palladium-catalyzed cross-coupling reaction of organosilicon reagents with organohalides, also known as the Hiyama coupling reaction (Scheme 1), is a useful synthetic tool for the formation of carbon-carbon bonds.[16]

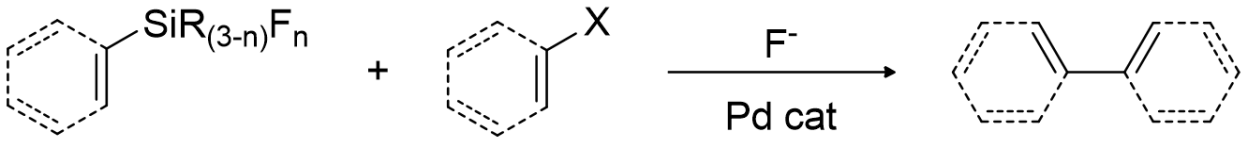

Scheme 1 Hiyama Cross-Coupling reaction

Relative to other organometallic compounds used in cross-coupling reactions (eg. SnR_3, Stille-Migita-Kosugi; $B(OR)_3$, Suzuki-Miyaura; Zn(R)(X), Negishi), organosilicon compounds are weak nucleophiles as a result of the low polarization of the Si-C bond.[17] The markedly inert character of these compounds is advantageous in synthesis, as they tolerate a wide variety of functional groups; however, their chemical stability makes them poor cross-coupling partners.[18] Early work by Hiyama showed that activation of organosilicon reagents can be achieved through use of a fluoride salt, such as NBu_4F (tetrabutylammonium fluoride, TBAF) or

$[(Me_2N)_3S]^+[F_2SiMe_3]^-$ (Tris(dimethylamino)sulfonium difluorotrimethylsilicate, TASF), resulting in a competent coupling reagent.[19] Hiyama proposed that fluoride activation of the organosilicon reagent allows for the *in situ* formation of a pentacoordinate organosilicon anion whose labile carbon-silicon bond is essential for the facilitation of transmetalation in the catalytic cycle (**Error! Reference source not found.**).[16,17,20,21]

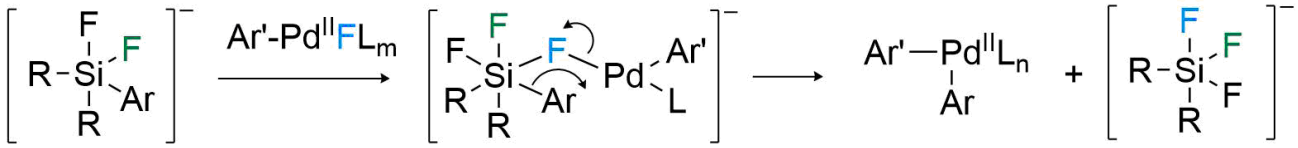

Scheme 2 Proposed transmetalation step in the Hiyama Cross-Coupling Reaction[20]

While this pentacoordinate silicon species is proposed to be the reactive species in the transmetalation step of the Hiyama reaction, there still remains little experimental data either confirming its presence or depicting the role it plays in transmetallation.[16,17,20,22–24] The overall lack of mechanistic evidence combined with the inherent anionic charge of the pentacoordinate silicon species made it an ideal candidate for mechanistic analysis by ESI-MS.

While initially we investigated the mechanism of the Hiyama reaction under catalytic conditions, as outlined in Scheme 3,[25] our preliminary findings led us to focus on just one component of the overall reaction: an examination of the reactivity between the fluoride source and the neutral fluorotriphenylsilane. It proved to be considerably more complicated than anticipated, and the results are very much a cautionary tale.

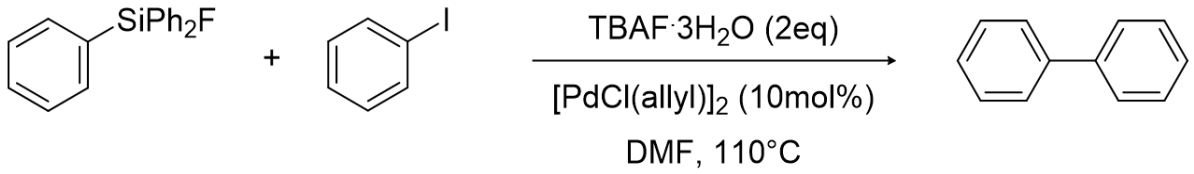

Scheme 3 Hiyama Cross-Coupling reaction of aryl iodides with fluorotriphenylsilane in the presence of 2 equivalents of TBAF and an allylpalladium chloride dimer catalyst.

2.2 Optimization of Conditions and Methodology for ESI-MS Analysis

Before embarking on a full study of the Hiyama reaction, we needed to establish parameters for the conditions employed. Hiyama reactions are generally carried out at high temperature (>100 °C) and in moderately coordinating polar aprotic solvents such as N,N-dimethylformamide (DMF), tetrahydrofuran (THF), or hexamethylphosphoramide (HMPA).[18,26] We had not previously employed such forcing conditions nor such a high boiling point solvent in PSI-ESI-MS studies; however, we found that with the appropriate source conditions (see experimental section) DMF proved to be a well-behaved solvent for electrospray ionization.[25,27]

While the PSI setup is inherently capable of handling high temperature reaction mixtures, over the years we as a research group have observed numerous unidentified contaminant peaks when analyzing reactions at elevated temperatures in the negative ion mode. For example, heating a 50:50 mixture of MeOH and MeCN to 80ºC in a PSI flask produces a spectrum like the one in Figure 2.1.

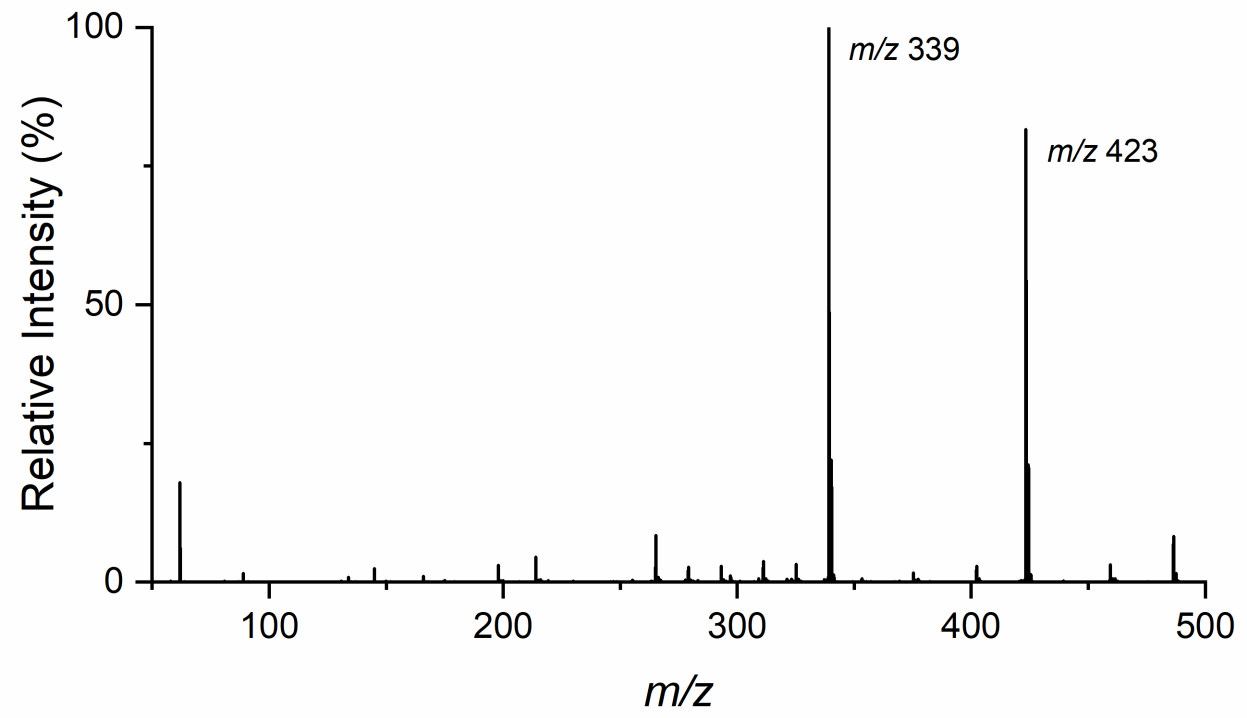

Figure 2.1 ESI(-) spectrum of a 50/50 mixture of MeOH and MeCN stirring at 80ºC in a standard PSI flask demonstrating the high relative intensity of the unidentified anionic contaminant species (*m/z* 339 and *m/z* 423).

As elevated reaction temperatures appeared to amplify the presence of these contaminants, we suspected that they may be originating from the rubber septa being used on the PSI flask. Natural rubber septa are present in most lab environments and one of the most common types we use are the Precision Seal® white rubber septa.[28] These septa are designed to be non-contaminating, advertised as being "low (1.9%) in solvent extractables, high density to prevent the effects of solvent degradation, with an upper heat limit of 85ºC and containing 0.19% volatile species. The septum is composed of standard rubber no. 1, accelerant, oxidizer, hard resin acid, anti-ager, lime carbonate, and dye agent". Normally, such species are present at low enough levels that they do not interfere with the reaction significantly; however, when studying reactions using sensitive methods such as mass spectrometry, the appearance of even trace

amounts of contaminant material can complicate mechanistic analyses by overlapping with and obscuring the low-intensity species of interest.

To attempt to identify these confounding contaminants, particularly the abundant *m/z* 339 and *m/z* 423 species, a sample was submitted for high resolution mass spectrometry analysis. Unfortunately, we had to purchase more septa before the sample could be prepared for analysis, and this new batch did not produce the *m/z* 423 species and therefore exact mass data for this ion was not obtained. High resolution mass spectrometry data was obtained for the *m/z* 339 species (Figure 2.2), and we determined that the exact mass of *m/z* 339.23274 corresponded to only one CHNO ion to within 1 ppm: $C_{23}H_{31}O_2^-$ (calc. *m/z* 339.232).[29] Given that we were running in the negative mode and were therefore expecting to see deprotonated species, we looked for a molecule corresponding to the molecular formula of $C_{23}H_{32}O_2$ with an acidic proton and 8 double bond equivalents (DBEs). Such a formulation pointed strongly to an aromatic compound - two benzene rings is 8 DBEs - and a phenol, to account for the high efficiency of ionization in the negative ion mode. By looking at common additives used in rubber manufacturing, we were able to find a likely candidate: 2,2'-methylenebis(4-methyl-6-tert-butylphenol) – also known as antioxidant 2246 – a common phenolic antioxidant used in rubber manufacturing.[30] To date, we have not been able to unambiguously identify the remaining species observed in the high resolution mass spectrum.

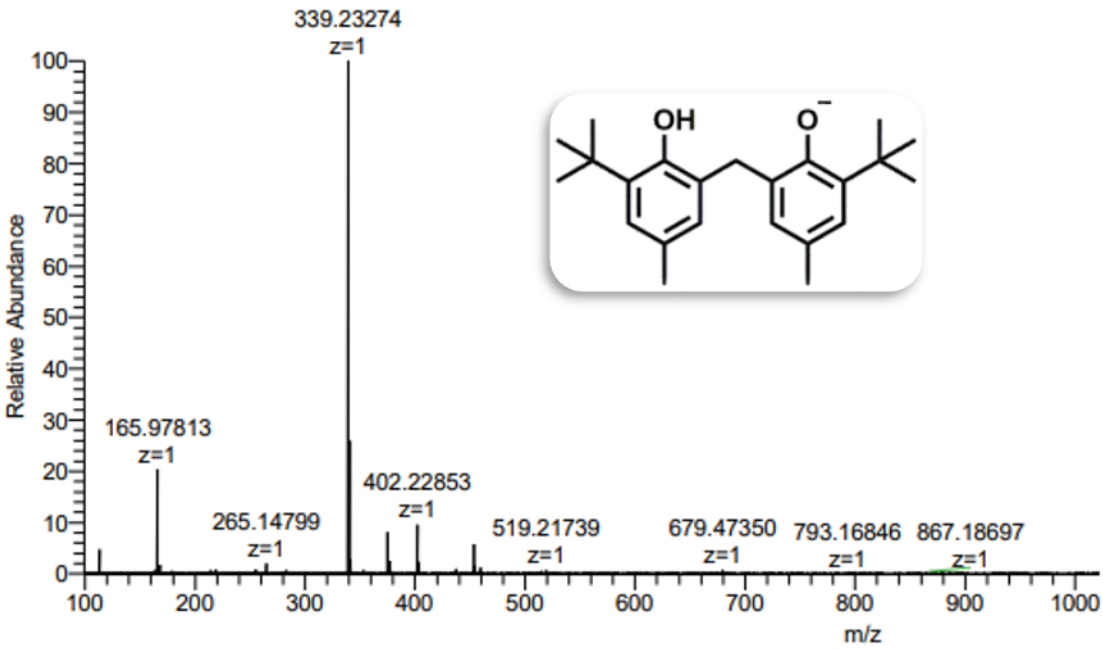

Figure 2.2 High resolution mass spectrum of observed rubber contaminant species in the negative ion mode. Inset: Structure of Antioxidant 2246 (2,2'-methylenebis(4-methyl-6-tert-butylphenol)), identified as the *m/z* 339 species.

Regardless of the identity of the contaminants, preventing their appearance in our analyses was important. The previous incarnation of PSI flask used a tap at the top to control the inlet of inert gas, with the ground glass joint covered by a septum below the condenser (Figure 2.3). With the joint below the condenser, leaching of contaminants from the septum occurred, in fairly high concentration, via the heated solvent. To minimize the presence of these species, we redesigned the PSI flask with the septum above the condenser, where the refluxing solvent is unable to reach it (Figure 2.3) and thus remedying the design flaw in the original piece of glassware.

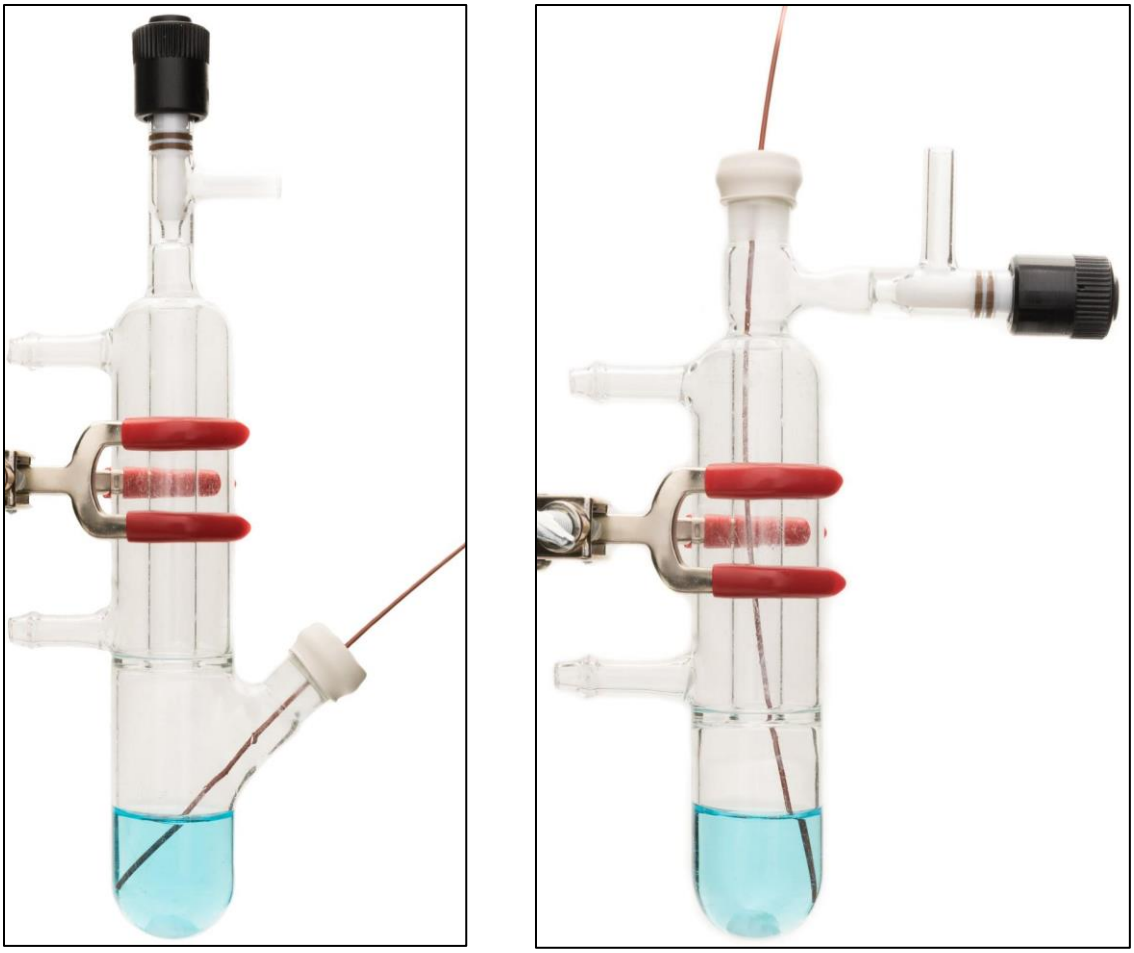

Figure 2.3 Left: first generation PSI flask. Right: re-designed second-generation PSI flask with ground glass joint above the condenser, positioned adjacent to the gas inlet tap.

This redesign proved quite effective for minimizing the contamination effect of the rubber septa. Analysis of a 50:50 mixture of MeOH and MeCN at 80ºC using PSI-ESI-MS reveals that the presence of the *m/z* 339 antioxidant is effectively eliminated (Figure 2.4). To further demonstrate the source and magnitude of this observed contamination, pieces of rubber septa were added to the reaction flask resulting in a dramatic ~1000× increase in intensity of the *m/z* 339 species (Figure 2.4, addition point labelled with an asterisk).

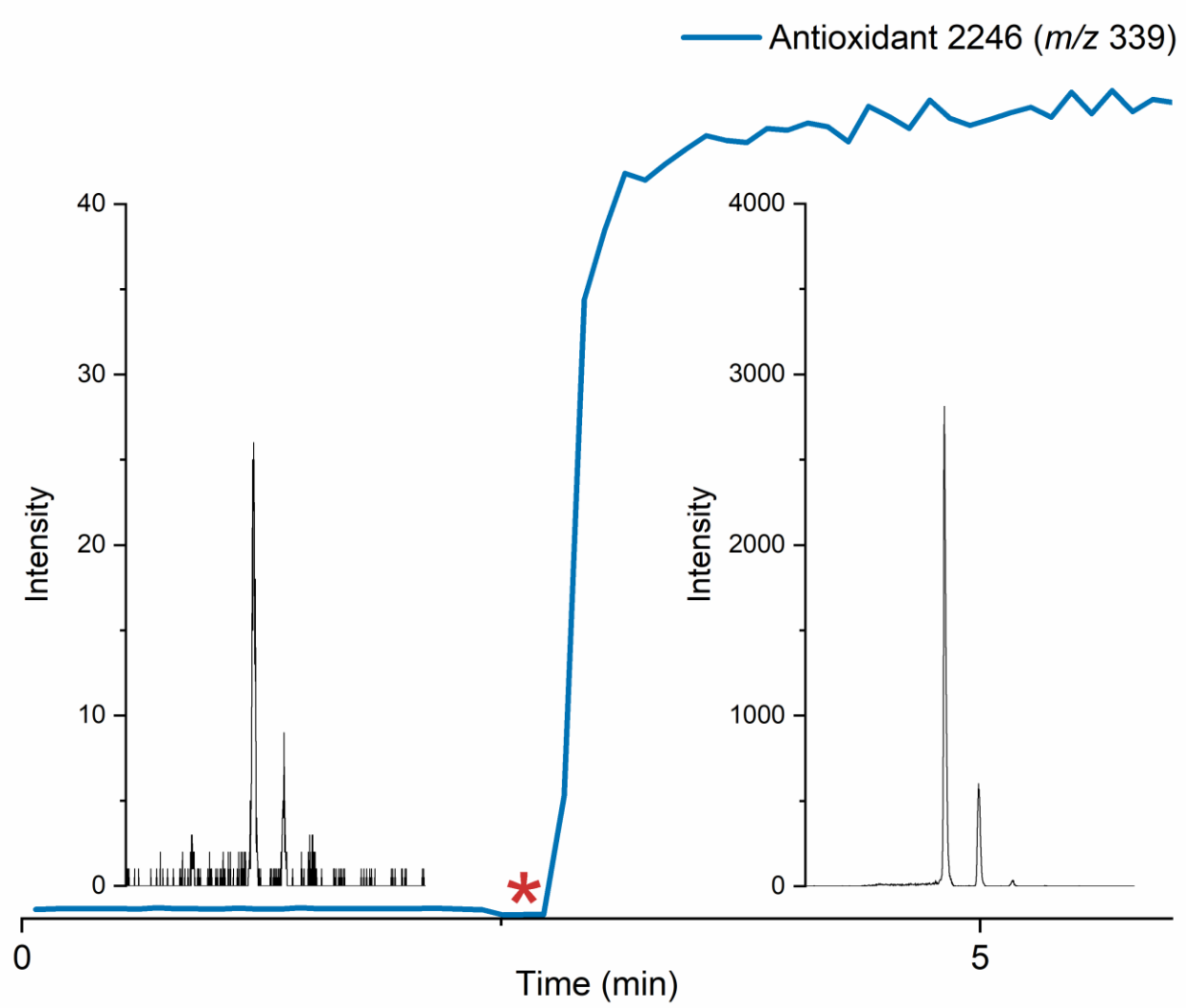

Figure 2.4 Presence of antioxidant 2246 (*m/z* 339) in a 50/50 mixture of MeOH and MeCN at 80°C using newly re-designed PSI flask before and after addition of rubber septa pieces. Insets show single scan intensity of *m/z* 339 before and after addition, and asterisk (*) signifies the point at which the septa were added.

After this problem-solving aside to minimize the appearance of the observed septum contaminants, we were able to proceed with the analysis of the Hiyama reaction.

Note: all PSI flasks in the group are now of the new design.

2.3 Results and Discussion

Electrospray Ionization Mass Spectrometry Results

The most commonly used fluoride activator for the Hiyama reaction is tetrabutylammonium fluoride (TBAF or NBu_4F), which is only commercially available in hydrate form due to the instability of anhydrous tetraalkylammonium fluoride salts.[31] Two equivalents with respect to the triarylfluoride are added to the reaction mixture, as per the conventional experimental protocol.[20]

When Ph_3SiF is combined with two equivalents of $[NBu_4]F$ in DMF at 110ºC, rapid formation of an anionic species at *m/z* 297 occurs, readily assigned as the pentacoordinate silicate $[Ph_3SiF_2]^-$. The MS/MS product ion spectrum (Figure 2.5) for this species shows unimolecular decomposition at high collision voltages only, breaking down to eliminate benzene ($Ph^- + H^+$) either through rearrangement or heterolytic Si-C bond cleavage.

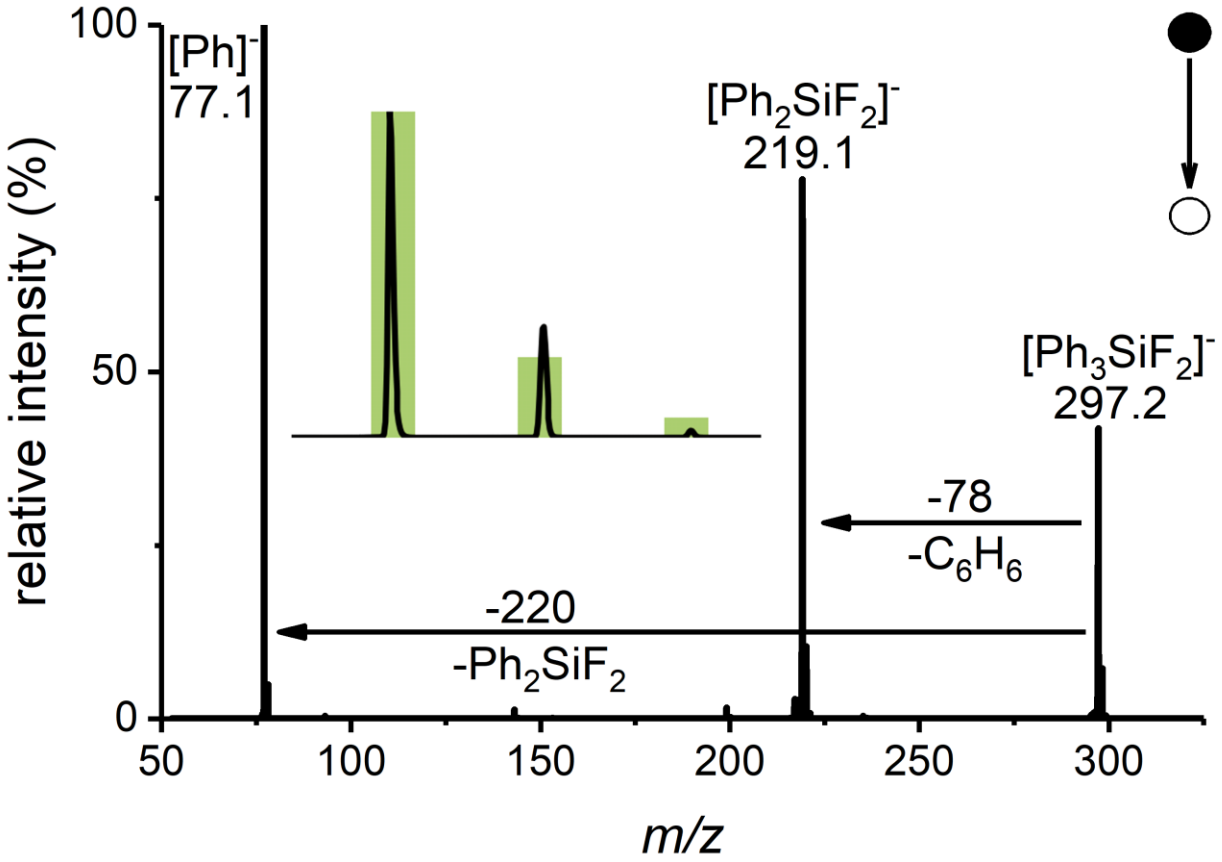

Figure 2.5 MS/MS product ion spectrum of $[Ph_3SiF_2]^-$. Inset: isotope pattern of the precursor ion (line experimental data, bars calculated).

Following the formation of the *m/z* 297 species, redistribution of the aryl groups is immediately initiated, and the temporal evolution of the observed species is shown in Figure 2.6.

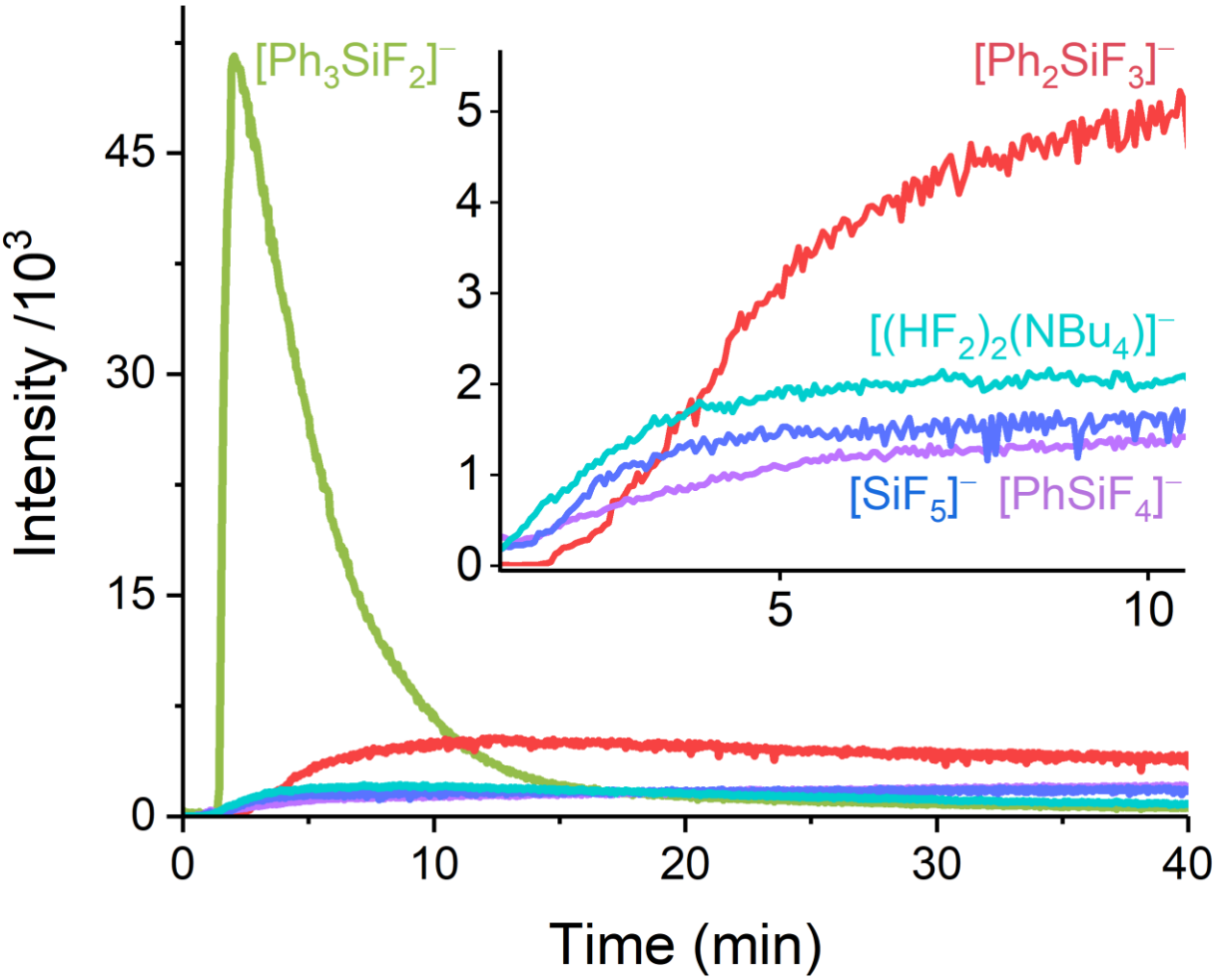

Figure 2.6 Temporal evolution of $[Ph_{(3-n)}SiF_n]^-$ and $[HF_2]^-$ during the addition of Ph_3SiF to two equivalents of TBAF in dimethylformamide at 110°C. Traces are averages of three replicates. Inset: expansion of lower abundance species.

The reaction between F^- and Ph_3SiF is extremely fast ($t_{½}$ < 45 seconds), given the near-vertical ascent of the line immediately following combination of reagents. The exchange reaction that consumes it is slower, with a half-life of approximately five minutes. Three other anionic pentavalent silicon species were observed as products: $[Ph_2SiF_3]^-$ (*m/z* 239), $[PhSiF_4]^-$ (*m/z* 181), and $[SiF_5]^-$ (*m/z* 123), whose identities were confirmed using MS/MS experiments and isotope

pattern analysis (Figure 2.7 and Figure 2.8)[a]. A fifth prominent species is also observed at *m/z* 320, which was identified as the aggregate species $[(NBu_4)(HF_2)_2]^-$ based on isotope pattern and MS/MS data (Figure 2.9).

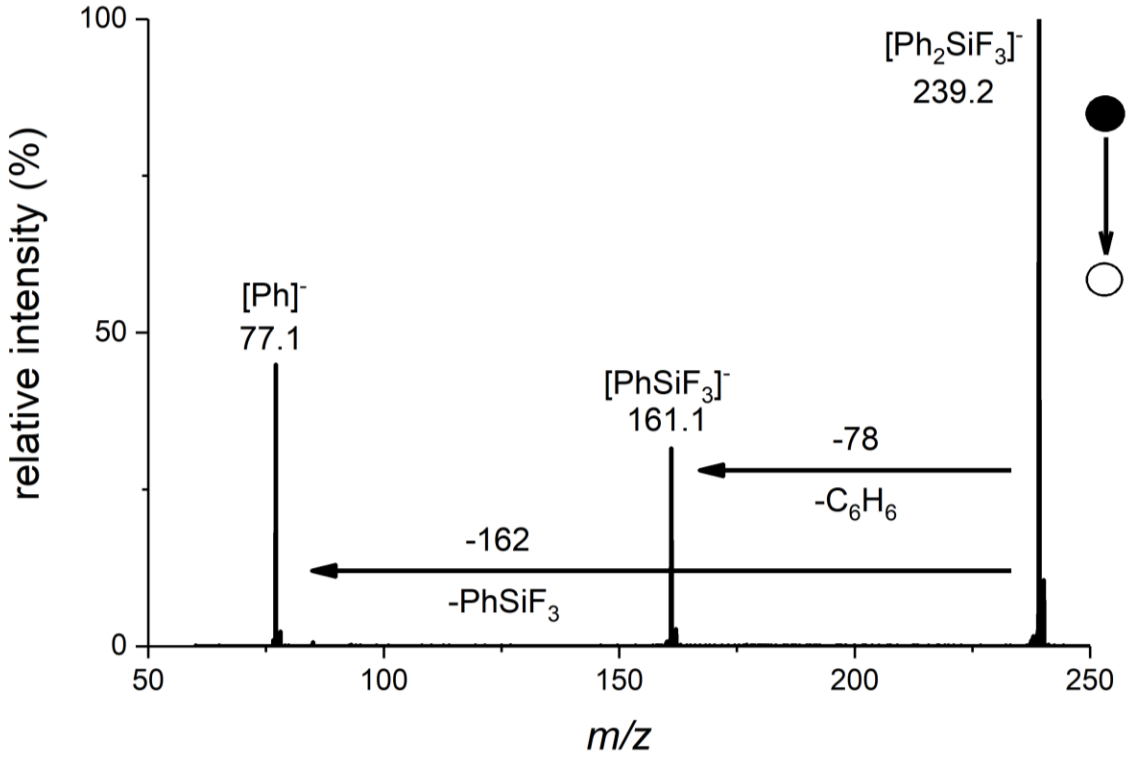

Figure 2.7 MS/MS spectrum of $[Ph_2SiF_3]^-$ (*m/z* 239)

[a] Note that MS/MS spectrum for SiF_5^- did not contain any useful information, as the *m/z* of the expected fluoride fragments falls below the instruments lower working mass range (*m/z* 50), and therefore was not included.

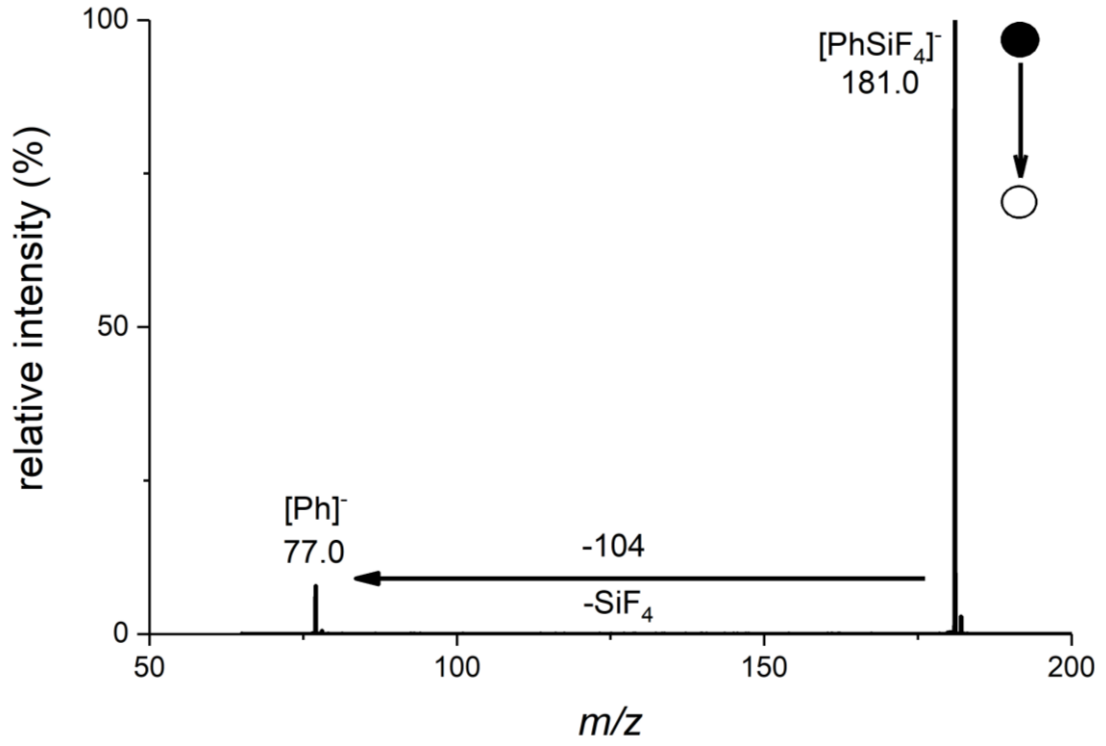

Figure 2.8 MS/MS spectrum of $[PhSiF_4]^-$ (*m/z* 181)

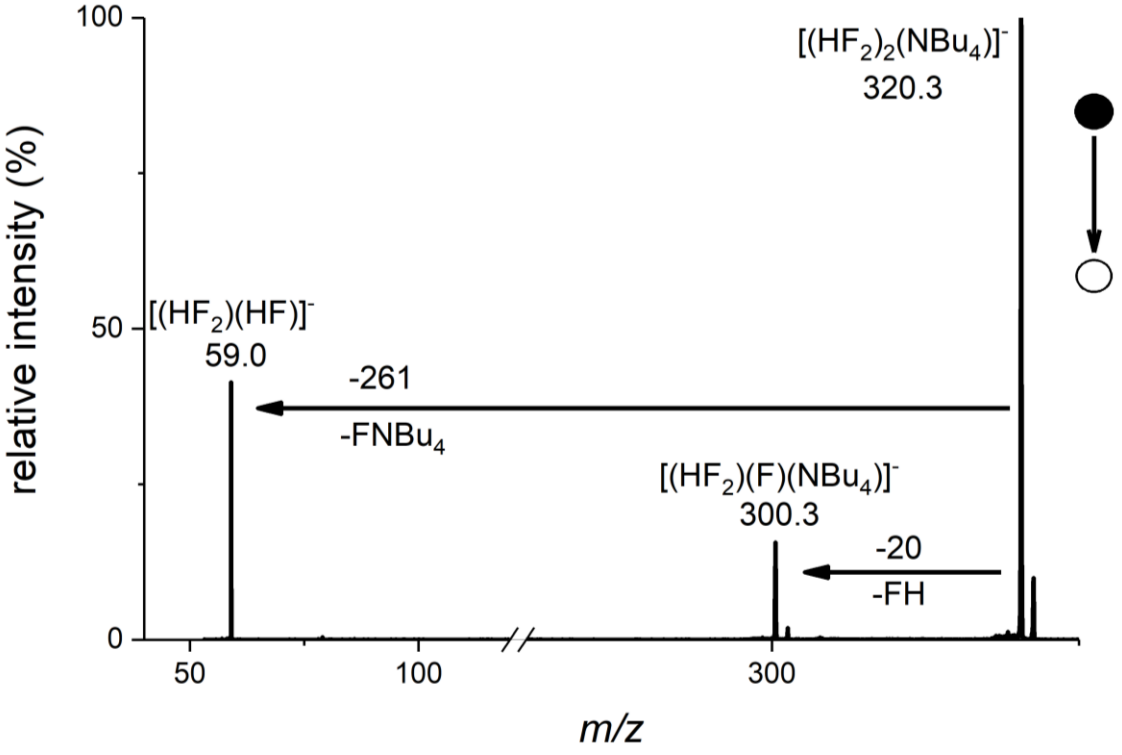

Figure 2.9 MS/MS spectrum of $[(HF_2)_2(NBu_4)]^-$ (*m/z* 320)

The traces shown in Figure 2.6 are averages of three replicates, as we observed variability in the relative intensities of the observed species when repeating the experiment. Qualitatively, the reaction behaved very similarly, in that the $[Ph_3SiF_2]^-$ always formed very quickly and disappeared with a consistent half-life of about 5±2 minutes (Figure 2.10); however, the relative abundance of the product species was considerably more variable (remaining error bar plots can be found in Appendix A, Figures. A.1-A.3).

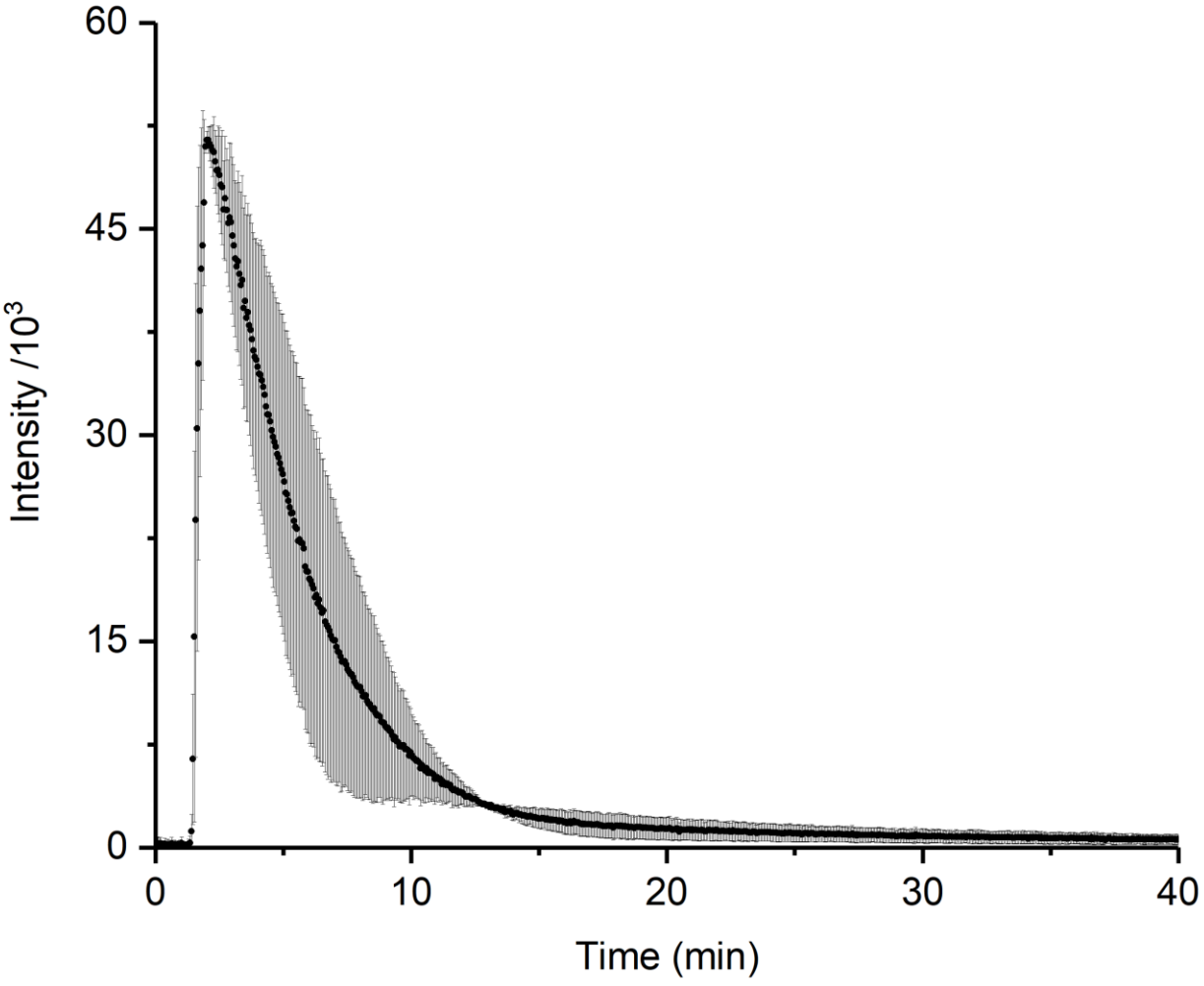

Figure 2.10 Error bar plot for the intensity of $[Ph_3SiF_2]^-$ (*m/z* 297) over time, data averaged from three replicates.

This variability from experiment to experiment we attribute to the reaction itself rather than any inherent erratic behavior in the PSI-ESI-MS methodology, which regularly produces traces with high reproducibility in other contexts.[32–34] One possible cause is the solvent, *N,N'*-dimethylformamide, whose hydrolysis into dimethylamine and formic acid occurs without catalyst at room temperature.[35] These decomposition products, even if present in only small amounts, may dramatically influence the rate and/or success of the reaction, especially if the exchange reaction is acid-catalyzed. Unfortunately, commercial TBAF cannot be obtained free of water, therefore the presence of water cannot be completely eliminated from the reaction mixture.[36] Nonetheless, the overall trend is clear in all experiments: within about 20 minutes, very little $[Ph_3SiF_2]^-$ remains in solution and the spectrum is dominated instead by fluorine-rich silicate species. Note that no $[Ph_4SiF]^-$ or $[Ph_5Si]^-$ is observed, so the mass balance of Ph is not preserved. It is possible that formation of tetraphenylfluorosilicates is disfavored on steric grounds, given that reaction of PhLi with Ph_3SiF produced a 4:3 mixture of Ph_4Si and $[Ph_3SiF_2]^-$, rather than the intended $[Ph_4SiF]^-$.[37] As such, we investigated whether neutral Ph_4Si is the invisible (to ESI-MS) sink for the "missing" phenyl groups. Under identical reaction conditions to our previous experiments, combining an authentic sample of Ph_4Si with two equivalents of NBu_4F resulted in the similar rapid disappearance of phenyl groups (Figure 2.11), indicating that Ph_4Si is not a secure reservoir of Ph groups.

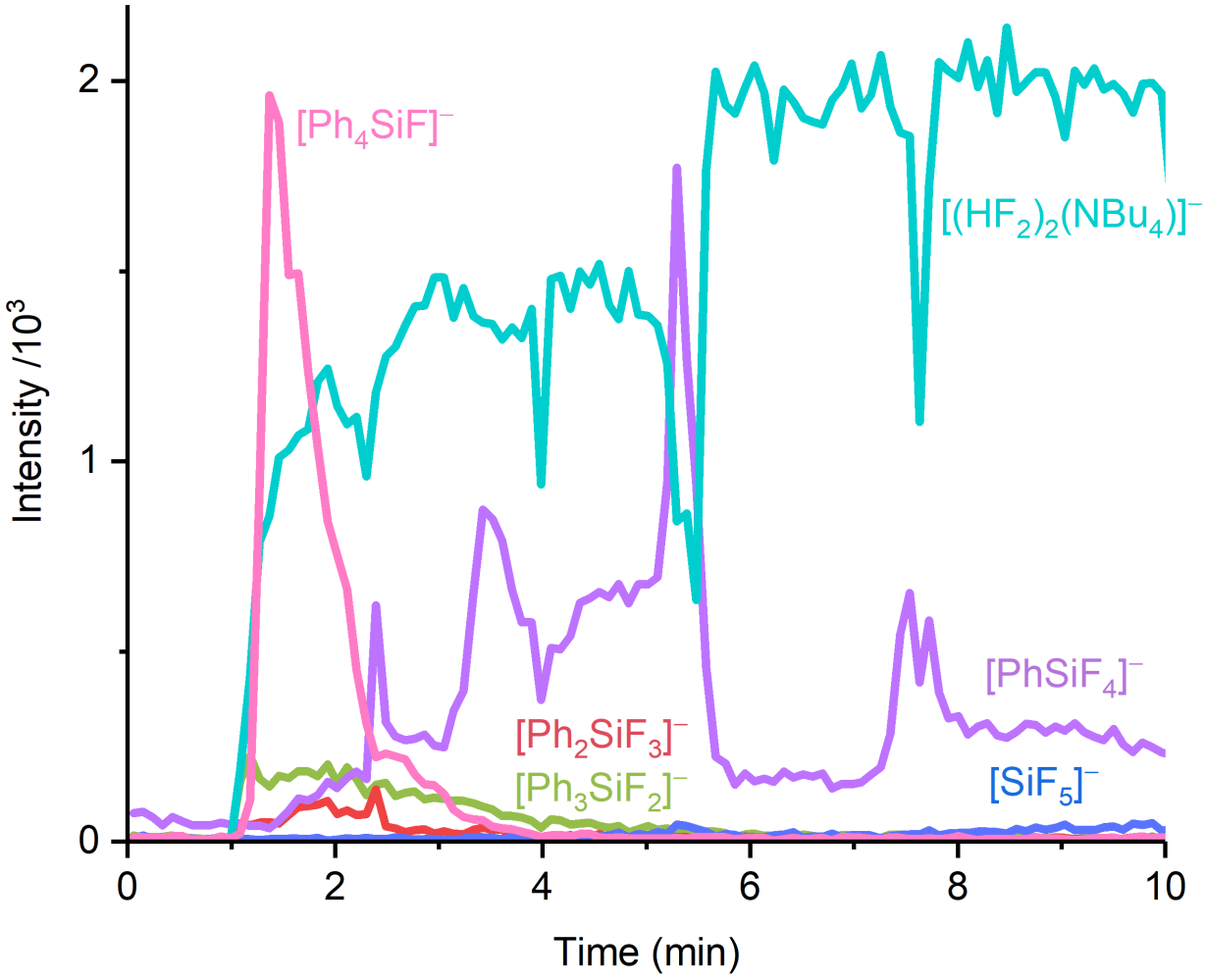

Figure 2.11 Temporal evolution of $[Ph_{(4-n)}SiF_n]^-$ and $[HF_2]^-$ during the addition of Ph_4Si to two equivalents of TBAF in dimethylformamide at 110°C.

Attempts to detect the presence of neutral species in the reaction mixture using Cold-EI GC-MS analysis were unfruitful; the results showed a complex chromatogram, dominated largely by solvent and column bleed peaks. While we did observe the presence of some unreacted Ph_3SiF, we were unable to find evidence of any other neutral silane species or potential phenyl reservoirs (such as Ph_4Si or biphenyl) from the data.

Multinuclear NMR Results

Because the phenyl group is not an informative handle for either proton or carbon NMR, we turned to $^{19}F\{^{1}H\}$ and ^{29}Si NMR to provide additional insights. Unfortunately, even through the use of distortionless enhancement by polarization transfer (DEPT), ^{29}Si NMR spectra could not be obtained for the reaction mixture (Appendix A, Figure A.4). The lack of detectable signal can be attributed to the mixture of products lowering the signal-to-noise and the signal being distributed across complex multiplets ($[SiF_5]^-$ would be a sextet, for example). Despite the lack of results from the ^{29}Si NMR experiments, spectra were successfully obtained using ^{19}F NMR, though given the low time resolution of the technique the reaction was carried out at room temperature rather than at the elevated temperatures used for ESI-MS. NMR Reference spectra (Appendix A, Figures A.5-A.7) were obtained for both Ph_3SiF ($^{19}F\{^{1}H\}$: δ -169 (d, $^{1}J_{F\text{-}Si}$ = 281 Hz), ^{29}Si: δ -4.37 (d, $^{1}J_{Si\text{-}F}$ = 281 Hz)) and TBAF·$3H_2O$ ($^{19}F\{^{1}H\}$: δ -143.1, -143.6).[36,38,39]

To follow the reaction using ^{19}F NMR, Ph_3SiF and two equivalents of TBAF·$3H_2O$ were combined in an NMR tube at room temperature and spectra were acquired at 0, 16, and 72 hours after mixing (Figure 2.12). The first spectra, acquired immediately after mixing, revealed the appearance of a new peak at -97.5 ppm, consistent with the mass spectrometric observation of rapid formation of $[Ph_3SiF_2]^-$. The doublet observed at -143 ppm arises because the spectrum is not proton decoupled and so coupling to the H of $[HF_2]^-$ occurs. A few small new peaks had grown in after 16 hours, and after 72 hours they had become appreciable and some were more abundant than the initial $[Ph_3SiF_2]^-$ species. The doublet at -143 had almost disappeared and a singlet at -144 grew in. This can be attributed to disappearance of the $[HF_2]^-$ and replacement by F^-, consistent with the growth of the signal at -105 ppm.

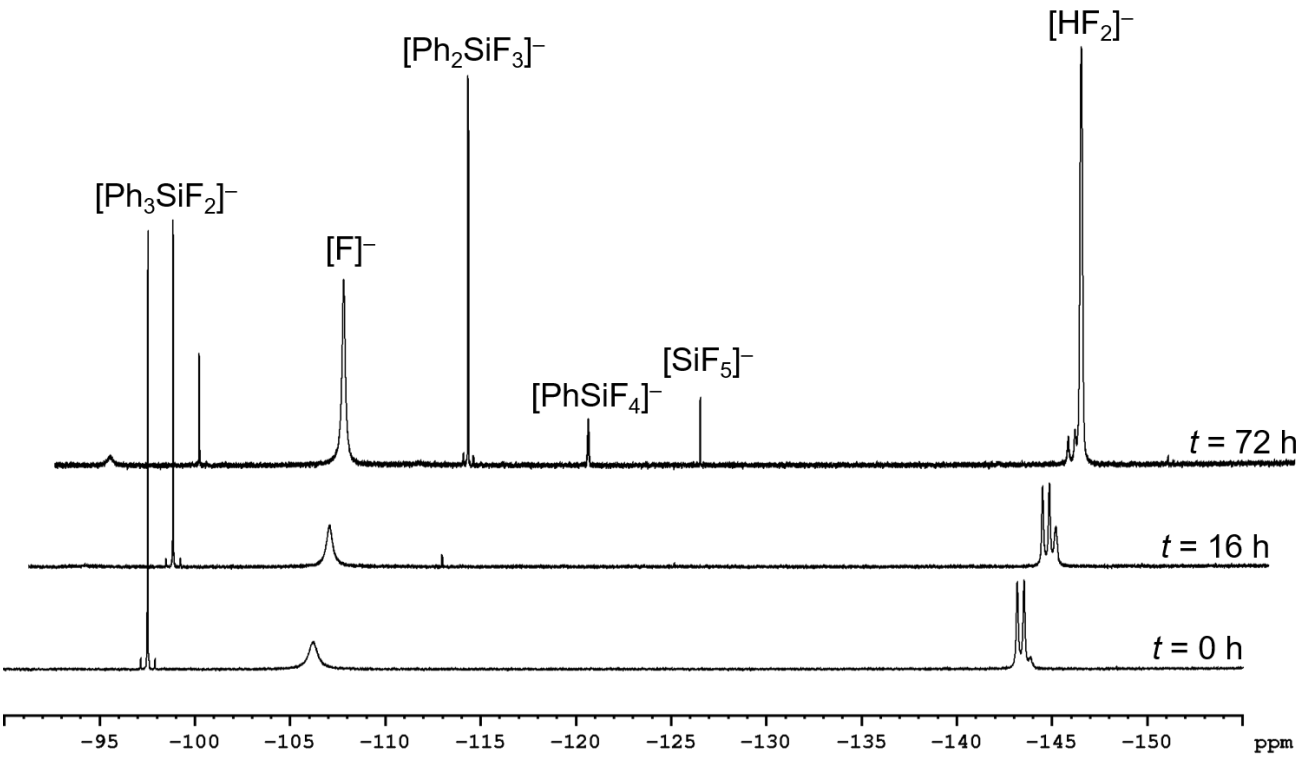

Figure 2.12 ^{19}F NMR of Ph_3SiF + 2eq TBAF·3H_2O in DMF acquired at 0, 16, and 72 hours after mixing at room temperature.

Literature values for the chemical shifts of some anionic silicon fluoride species are available, albeit in different solvents. Literature values for the three fluorophenylsilane species are similar to our observed values, with $[Ph_3SiF_2]^-$ being reported at -95 ppm ($CFCl_3$)[40], $[Ph_2SiF_3]^-$ at -111 ppm (d_6-acetone/vinyl chloride mixture),[41] and $[PhSiF_4]^-$ at -119 ppm (C_6H_6/CH_2Cl_2 mixture).[42,43] $[SiF_5]^-$ is reported to appear at -137 ppm (we did not observe any peaks in this region), and $[SiF_6]^{2-}$ at -127 ppm (C_6H_6/CH_2Cl_2 mixture)[42] making it a possible candidate for the peak at -125 ppm.

2.4 Conclusions

The application of real-time ESI-MS to a high temperature reaction of Ph_3SiF and fluoride revealed rearrangement of the rapidly (<10 s) formed $[Ph_3SiF_2]^-$ ion to generate a range of more highly fluorinated silicate ions of the form $[Ph_nSiF_{5-n}]^-$ (n = 0-2) over a period of minutes. Confirmation of the rearrangement came from room temperature ^{19}F NMR studies. Neither of these techniques, nor ^{29}Si NMR or ^1H NMR or GC-MS were informative regarding the fate of the "missing" phenyl groups. The observation of rearrangement itself is significant for reactions that utilize $[Ph_3SiF_2]^-$ ions (most notably the Hiyama reaction), because the rearrangement leads to lower availability of Ph for cross-coupling. Further elucidation of the details of the rearrangement will likely require the use of a triarylfluorosilane with a good ^1H NMR handle (e.g. the *para*-tolyl analogue, not commercially available).

2.5 Experimental

Unless otherwise noted, all manipulations were performed under an inert atmosphere (N_2), using conventional Schlenk techniques and oven-dried glassware where appropriate. ACS grade DMF (Caledon) was dried and stored over 4Å molecular sieves, and sparged with nitrogen for 15 minutes before use. Commercially obtained Ph_3SiF (TCI Chemicals, >97.0%) and $[CH_3(CH_2)_3]_4NF{\cdot}3H_2O$ (Sigma-Aldrich, >97.0%) were used without further purification and stored under nitrogen.

ESI-MS spectra were collected using either a (i) Micromass Q-ToF *micro* hybrid quadrupole/time-of-flight mass spectrometer (QtoF) or a (ii) Waters Acquity triple quadrupole

detector with a Z-spray ionization source (TQD)[b], in the negative mode using pneumatically-assisted electrospray ionization. Capillary voltage: 3000 V. Cone voltage: 15V. Source temperature: 110°C. Desolvation temperature: 220°C. Cone gas flow: 200 L h^{-1}. Desolvation gas flow: 200 L h^{-1}. Collision Energy: 2 V. MCP detector Voltage (QToF): 2400V. Phosphor detector gain (TQD): 470 V. MSMS experiments were performed with a collision energy between 2-30 V with an argon collision gas flow rate of 0.1 mL/hr.

The general reaction procedure for the PSI-ESI-MS experiments was as follows: a solution of tetrabutylammonium fluoride trihydrate (0.0158 g, 0.0501 mmol) was dissolved in 4.50 mL *n*,*n*-dimethylformamide in the specially designated PSI reaction flasks. The reaction mixture was heated to 110°C (regulated using a thermocouple) and stirred for the course of the reaction. A solution of fluoro(triphenyl)silane (0.0070 g, 0.025 mmol) in 0.50 mL *N*,*N*-dimethylformamide was then added to the reaction flask via syringe.

All NMR spectra were acquired on a Bruker AVANCE 360 MHz spectrometer. Samples were prepared at a 25mM (Ph_3SiF) concentration, in d_6-DMSO ($^{19}F\{^1H\}$, ^{29}Si) or in non-deuterated DMF with a d_6-acetone coaxial insert (^{19}F). Coupling constants (J) are expressed in hertz (Hz), chemical shifts (δ) are reported in parts per million (ppm) at ambient temperature.

High resolution accurate mass data was acquired using a Thermo Exactive Orbitrap LC-MS with an ESI ionization source. Mass accuracy was kept below 1 ppm using internal lockmass. 30 ul of the sample was injected in direct infusion mode and at a flow rate of 30 ul/min 1:1 isopropyl alcohol/water mix.

---

[b] differs from QtoF only in that it has a quadrupole in place of the ToF

Cold EI GC/MS data were obtained using a PerkinElmer AXION iQT GC/ MS instrument equipped with a Clarus 680 GC. The injector is programmable split/splitless injector connected with a PerkinElmer Elite™-5MS (length 30 m, inner diameter 250 mm, film thickness 0.25 µm) non-polar capillary column cross-bonded with 5% diphenyl/95% dimethyl polysiloxane. Injector: 290°C, Source: 200°C, Transfer Line: 250°C, Oven: 30°C. The reaction mixture was quenched, filtered through basic alumina, and diluted to an appropriate concentration using DMF.

Part II: Alternative Strategies for Molecular Modelling to Improve Comprehension of Molecular Geometry and Enhance Representational Competence

Chapter 3. Introduction to Molecular Modelling and Representational Competence

3.1 Representational Competence and Chemistry

In the words of the eminent chemist Richard Zare "chemists are highly visual people who want to "see" chemistry and to picture molecules and how chemical transformations happen".[45] At a molecular level, chemical phenomena are often imperceptible; however, experienced chemists have the ability to picture chemistry in their minds by visualizing molecules and their interactions. While chemists are able to think about molecules in three dimensions, they rely on a variety of visual-spatial representations, such as structural diagrams or reaction equations to communicate their ideas and teach concepts.

As representations are fundamental to discourse in chemistry, representational competence has been identified as a crucial contributor to success within the field.[46–49] Stieff et al. (2016), describe the term *representational competence* as a "discrete set of skills for

constructing, selecting, interpreting, and using disciplinary representations for communicating, learning, or problem solving."[50]

It is the set of skills that, for example, allows an experienced chemist to spatially interpret a molecular structure and predict reactivity. Research in science and chemical education highlights the importance of representational competency for learning a wide range of concepts taught in general chemistry, organic chemistry, inorganic chemistry, group theory, and biochemistry.[51–54] Some of the most fundamental concepts and theories taught to undergraduate chemistry students require them to generate, interpret, and fluently translate between a variety spatial representations, such as the ones shown in Figure 3.1. These are tasks that novice chemists often find to be very challenging,[55,56] and since these skills are heavily relied upon throughout their degree it may be one of the most significant conceptual hurdles for budding chemists to overcome.[57]

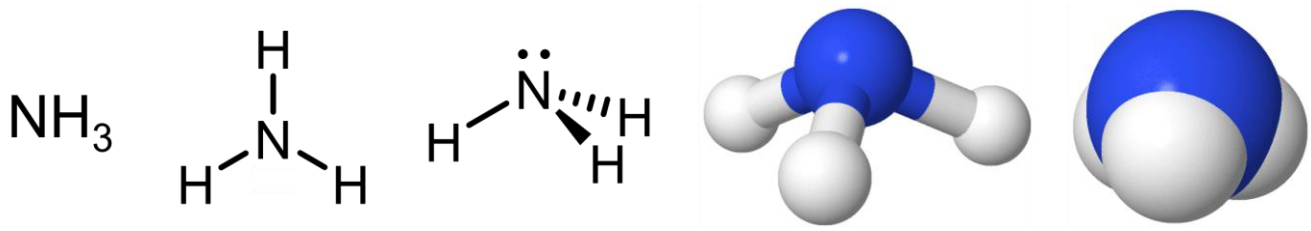

Figure 3.1 Example of different possible visual-spatial representations for an ammonia molecule

3.2 Concrete Models for Promoting Representational Competence in Chemistry

Given the importance of representational competence skills in chemistry, discipline-specific educational strategies that work to improve these fundamental skills may lead to improved student achievement in chemistry.

Activities that incorporate the use of molecular modelling tools, both virtual and concrete, are a common strategy utilized to improve students' representational competence and teach concepts where the visualization of three dimensional objects is necessary. Concrete hand-held models have been identified as being particularly beneficial for learning to perform tasks such as translating between representations, as being able to physically manipulate three-dimensional models helps reduce cognitive load – leading to improved learning.[58]

One popular and long-standing version of the concrete model is the conventional ball and stick model kits, often required in first and second year chemistry courses. There are many commercial molecular models available, including HGS, Cochranes, Molymod, and Molecular Visions, and while considered to be highly resilient and powerful, they are not without their limitations.

As part of a 2016 study by Stieff et al., a group of 234 introductory organic chemistry students were asked a series of questions regarding their usage of course required model kits. Interestingly, while 53% of students indicated that they believed they were useful for visualizing, interpreting, and relating molecular representations, a large majority (79%) of students indicated having rarely or never used the model kits they had purchased to support their learning or problem solving.[50] Student surveys revealed two key factors contributing to the low frequency of model use: (1) students felt the model kits were too time consuming to be practical, and (2) students found the model kits confusing to use and the relationship between the models and the molecular representation was unclear. These findings were consistent with those of a 2012 study by Stull et al.,[59] who found that while concrete models improved performance on the task of translating between representations used in organic chemistry, very few students chose to use them, citing an inability to use them effectively as one of the key factors. Students in this study

were often unable to effectively establish correspondence between the models and the diagrammatic representations, and some indicated that they found the models to be too complex or couldn't remember the conventions for assembly. The findings presented in both these studies supported the conclusion that while concrete models are beneficial for improving representational competence, in particular the skills associated with translating between molecular representations, there are clearly barriers preventing students from employing model kits effectively.

In first year chemistry, these commercially available kits are often employed for teaching novice chemists molecular geometry and VSEPR theory; however, they can be expensive and are often unnecessarily complex for the concepts taught at this level. Over the years, creative educators have developed methods for constructing physical models out of a wide range of media including (but not limited to): whiteboard markers,[60] beads and rods,[61] snap hooks and latex tubing,[62] circular magnets,[63] bar magnets and Styrofoam balls,[64] festive trees,[65] Styrofoam balls with Velcro strips,[66] and plastic globes,[67] coffee-stirrers,[68] and clay models and kite kits.[69] Many of these examples utilize inexpensive and readily available materials, often making them a cost effective method for construct models; however, constructing accurate representations can be challenging, and adding a new type of representation for students to interpret may further hinder students ability to effectively establish correspondence between existing representations.

3.3 Overview: Chemical Education Research

Based on the studies outlined in the preceding section, it is clear that early breakthroughs in understanding and appreciating molecular structure in three dimensions during first year chemistry will give students a firm foundation upon which to build higher level skills, but that

doing so presents some challenges, which we wanted to address through the development of a new strategy for creating molecular models. Our objective was to create a fresh and unique way of creating molecular models for the teaching molecular geometry in first year chemistry that would not only improve student comprehension of the material, but also help foster representational competence. We wanted to design a cost-effective process of constructing models that is not only fun and engaging, but simple enough to be accessible to students while still yielding high quality and scientifically accurate models. In the following sections, the development and application of two different approaches for generating molecular models for the teaching molecular geometry and VSEPR theory in first year chemistry is reported. Chapter 4 details a method for the application of handheld 3D printing pens for producing models from ABS plastic. In Chapter 5, the development of laser-cut acrylic model kits is detailed, as well as the design and results of a quantitative study aimed at assessing their effectiveness for improving representational competence and comprehension of molecular geometry.

Chapter 4. Handheld 3D Printing Pens

4.1 Introduction

3D printing technology has taken off in recent years, with 3D printed models being applied to the teaching of a wide range of topics in chemical education including: symmetry and point group theory,[70] protein domains,[71] unit cell theory,[72] orbital theory,[73–77] and structure-energy relationships.[78–80] A recent development in 3D printing technology is the handheld 3D printing pen, a device that extrudes hot plastic at a constant rate at a point in three dimensional space defined by the operator. (Figure 4.1)

Figure 4.1 Hand-held 3D printing pen

Applying this technology in the teaching of molecular geometry is potentially a valuable way to facilitate student understanding of molecular structure by adding a third dimension to a student's ability to draw molecules. We envisioned that by being able to "draw" the molecules in three-dimensions, it would help foster representational competence by allowing a student to physically relate a two-dimensional drawing with a three-dimensional model. Not only could this be a fun and engaging learning exercise for students, but the students could also keep their models afterward as the raw material, ABS plastic, is inexpensive.

4.2 Method

Novices to the 3D printing pen find it difficult to manipulate the pen accurately in three dimensions, and even experts usually generate 3D models by drawing 2D sections and assembling them together to make the final model. To streamline the drawing process for students, a 2D template was designed (Figure 4.2). Students are then able to simply trace over the template with the 3D printing pen, eliminating the need for strong artistic skills to produce quality models.

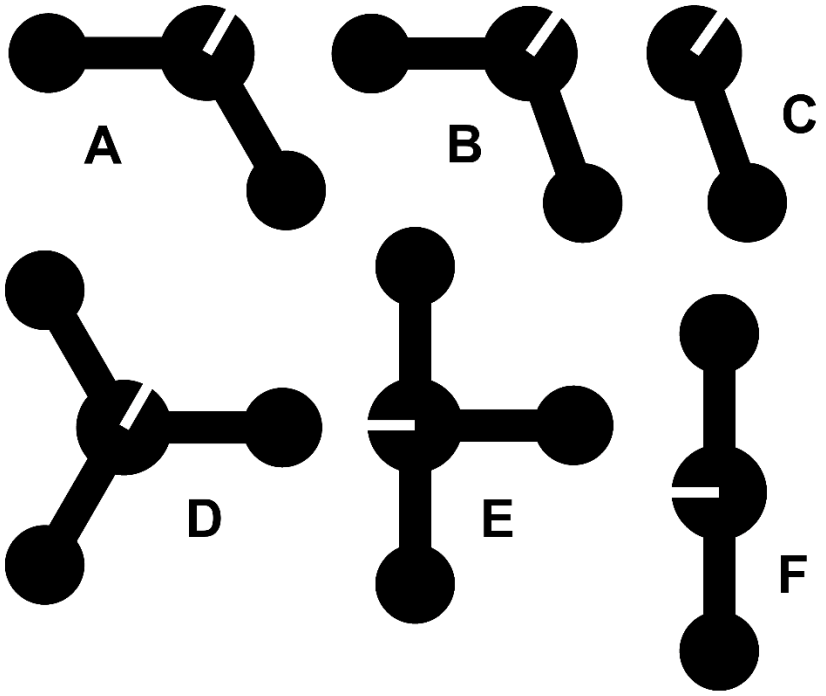

Figure 4.2 Two-dimensional templates. Linear = F (without notch). Trigonal planar = D (without notch). Bent (120°) = A (without notch). Tetrahedral = B + B. Trigonal pyramidal = B + C. Bent (109.5°) = B (without notch). Trigonal bipyramidal = D + F. Seesaw = A + F. T-shaped = E (without notch). Octahedral = E + E. Square pyramidal = E + F. Square planar = F + F.

We found that the best results were achieved when the user drew the circles for the atoms first, then joined them together by drawing in the bonds (Figure 4.3a), and finally coloured in both sides (Figure 4.3b) - a process that not only makes them more visually pleasing, but also adds strength to the model.

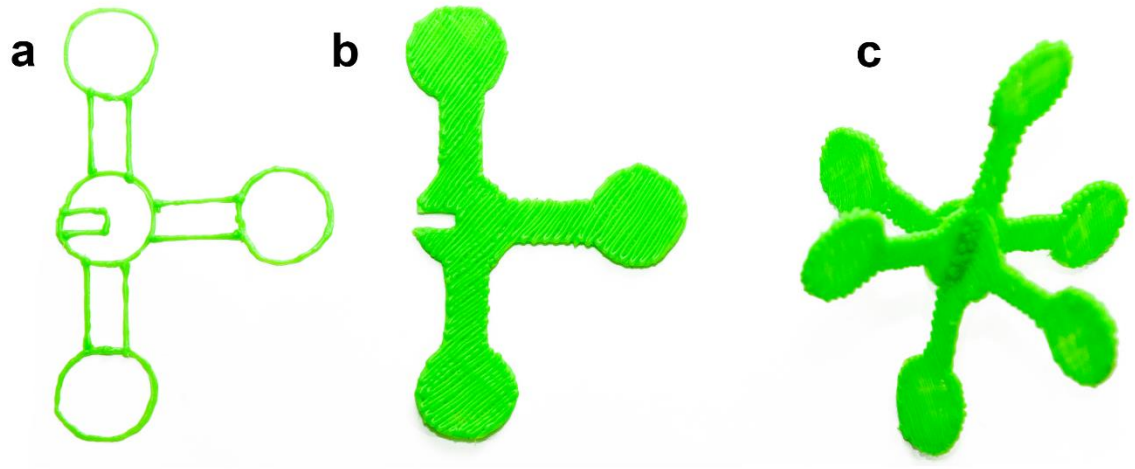

Figure 4.3 The three stages of the octahedral model construction from the template: (a) outline, (b) infill, (c) assembly.

The resulting shapes obtained using the 2D digital template were designed to be like puzzle pieces, where the students would trace two pieces with the 3D printing pen and then combine them into the corresponding molecular shape. The student would then hold the pieces in place and affix them together using the printing pen. For example, to produce an octahedral model, students would draw two copies of the T-shaped template (Figure 4.3b) and then join them together and fix them into place using a little extra plastic (Figure 4.3c). The end result is a series of beautiful, brightly-colored 3D models of the basic VSEPR shapes (Figure 4.4).

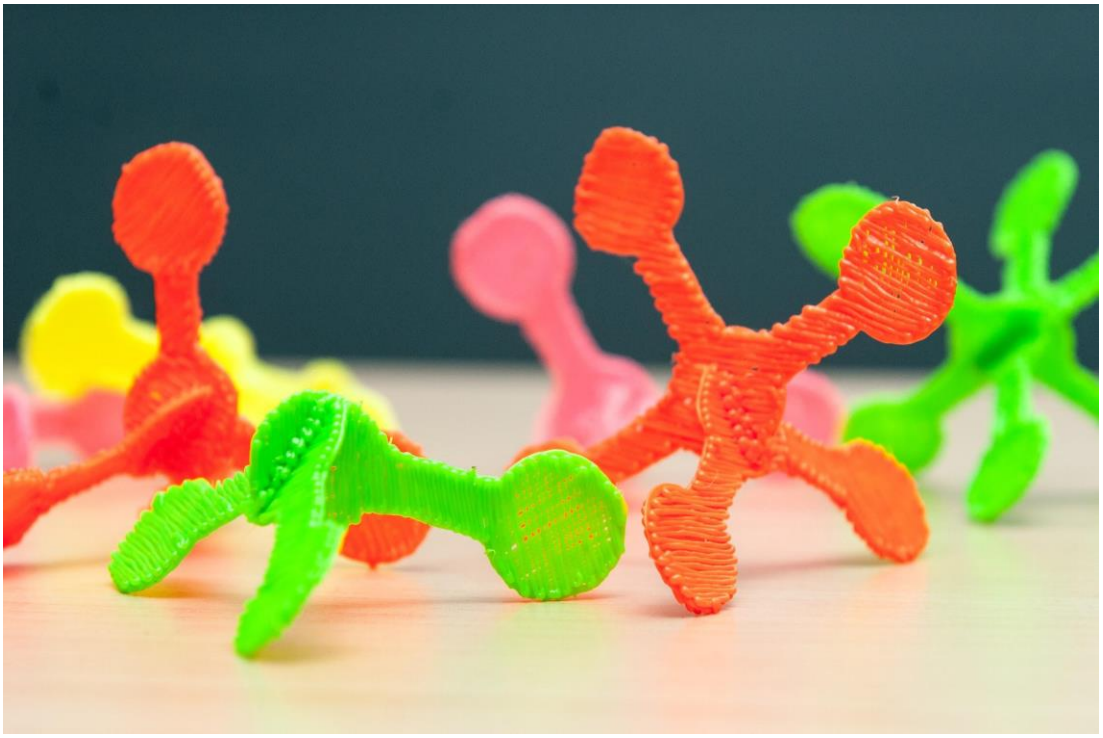

Figure 4.4 Sample of the molecular models produced using handheld 3D printing pens

The key to avoiding ink transfer into the plastic and the resulting discoloration of the models was to place a piece of paper on top of the template and trace directly on this blank top layer. Attempts were made to use glass and acrylic sheets in place of paper as a top layer, but the plastic did not adhere well enough to either to enable a high success rate.

4.3 Results and Discussion

There are 13 commonly encountered VSEPR geometries, but six have all of their atoms in the same plane and are the least in need of 3D representation: linear (2 electron domains[c] and

[c] It is noted that the terminology “electron domain” refers to an electron dense region around the central atom, arising due to the presence a lone/nonbonding pair or a bond (of any bond order).

5 electron domains); bent (120° and 109.5°); trigonal planar; T-shaped and square planar. That leaves six that require a genuine three-dimensional understanding: trigonal pyramidal, tetrahedral (4 electron domains), seesaw, trigonal bipyramidal (5 electron domains), square pyramidal, and octahedral (6 electron domains). Interestingly, when we let our test class have free rein to draw whatever they liked the majority chose to draw a trigonal bipyramid, perhaps because this was the only one of the five basic VSEPR shapes that required two different components. The test class, consisting of 20 first year students working in pairs, found constructing the models to be a fun, but challenging and time-consuming task, producing only one or two good quality models in the allotted 60 min (Figure 4.5).

Figure 4.5 Sample of molecular model produced by first year student using handheld 3D printing pen

This demonstrated that the learning curve associated with manipulating the pen accurately and the time required to draw a structure is sufficiently high that this exercise would need to be limited in a laboratory setting to students each being tasked with drawing a different molecule. The mechanical integrity of the produced models is also a potential drawback, as the models are relatively fragile and would probably not hold up to a day spent rolling around in a backpack. The mechanical integrity of the models is dependent on the amount of plastic used. Another consideration is the safety of using the 3D printing pen, as the tip of the pen reaches a

temperature of 240 °C (on the “high” setting), which does present a potential burn hazard for students using the pen; however, with proper instruction and supervision, this hazard should be minimal.[81] While these limitations make the technology difficult to deploy in an undergraduate laboratory, in the correct setting, hand-held 3D printing pens are a potentially useful tool for the teaching of molecular geometries and VSEPR theory and represent a fresh and unique way for students to learn about these concepts.

Chapter 5. Development and Assessment of Laser-Cut Acrylic Model Kits for the Teaching of Molecular Geometry

Previously we reported the application of handheld 3D printing pens to the teaching of VSEPR theory, where students could "draw" and assemble the 3D molecules themselves. While these pens were fun to use and created visually attractive molecular models, we found that the pens were slow, unreliable, and had a sufficiently high learning curve associated with accurate manipulation.[44] However, we realized that the 2D templates we had constructed to help these students could be deployed in another context, and we decided instead to cut the pieces out of transparent acrylic plastic using a laser cutter. This resulted in perfectly cut, beautiful models that snap together in seconds and that are inexpensive enough that the students not only can construct them in the lab but can also take them home for use as study aids.

5.1 Laser-Cut Acrylic Model Kits

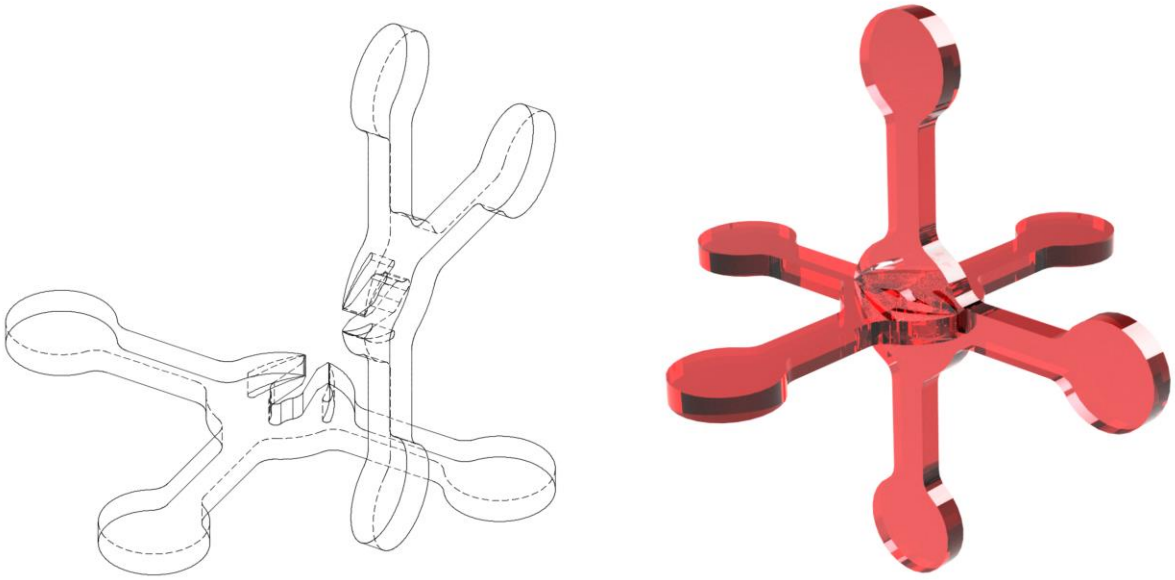

Figure 5.1 Drawing showing two identical pieces (left), and rendering of the two pieces after joining them together to form the press-fit model (right).

The 2D shapes (Figure 5.1) were laser cut from coloured transparent acrylic plastic (3 mm cast acrylic, purchased in 4’ × 8’ sheets and cut to the bed size of the laser cutter) by Sean Adams using the Chemistry departments’ Trotec 130 W Speedy 360 laser-cutter. The pieces were designed with a slit either side of the main notch which allows for variance in material thickness, ensuring a snug fit between all the pieces so that the models hold together firmly, but can also be easily dismantled. The plastic pieces were designed to be interlocked, where the students would combine the appropriate 2D pieces into the corresponding molecular shape. Each kit contains 26 acrylic pieces which can be assembled into 13 molecular shapes, color-coded by the number of electron domains (Figure 5.2). The approximate material cost CAN$2 per kit, inexpensive in the context of the costs of the first-year laboratory program.

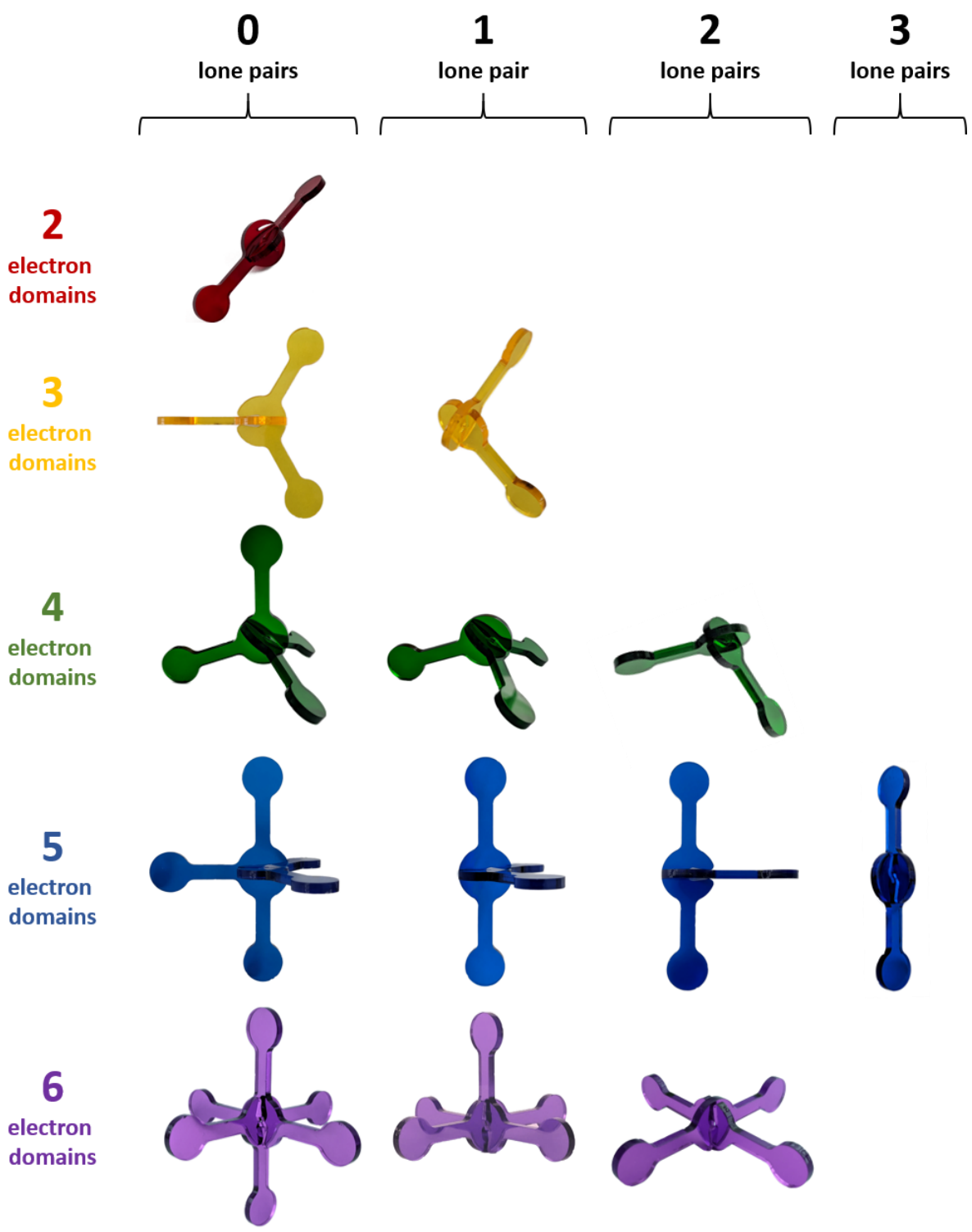

Figure 5.2 Complete set of laser-cut acrylic pieces, color coded by number of electron domains (nED). (a) Red (2ED): linear. (b) Yellow (3ED): bent (120°), trigonal planar. (c) Green (4ED): bent (109.5°), trigonal pyramidal, tetrahedral. (d) Blue (5ED): linear, T-shaped, seesaw, trigonal bipyramidal. (e) Purple (6ED): square planar, square pyramidal, octahedral.

5.2 Quantitative Assessment of Efficacy – Study Design

To assess whether the laser-cut models facilitated enhanced representational competence and improved comprehension of molecular geometry, we designed a set of surveys for first year chemistry students to complete before and after the laboratory exercise where they used the models. These surveys consisted of two parts: the assessment portion, primarily designed to evaluate student representational translation ability, and the questionnaire portion, intended to gauge the students' opinion regarding the models and their effectiveness. This section will detail the methodology and design of the study, describing the context, participants, procedure, and statistical analysis.

5.2.1 Context

Molecular geometry and VSEPR theory are part of the Chemistry 101 curriculum at the University of Victoria. These concepts are taught through a series of in-class lectures followed by an in-lab exercise designed to compliment the material and allow students to get hands-on experience with using molecular models to problem-solve. This study is limited to the molecular model kits themselves; the laboratory exercise, as outlined in the Chemistry 101 manual[82], was not within our sphere of influence.

The study was conducted over a three-year period where different methods were tested, the details of which are summarized in Table 5.1. In Year 1, no changes were made to the original laboratory exercise - where Chem 101 students were asked to construct a series of molecular models using a combination of polystyrene balls (atoms), toothpicks (bonding pairs), and bent pipe cleaners (lone pairs) - as we wanted to acquire control data to compare our new methodology. In Year 2, we replaced the Styrofoam ball kits with the laser-cut acrylic model

sets. In Year 3, the laser-cut acrylic model sets were used, in conjunction with a take-home exercise (in lieu of a laboratory exercise, see section 5.3.3 for more details) with the material supported by an in-class lecture where the students brought along their model kits.

Table 5.1 Summary of methods used in each year of the study

	Model Type	Activity Type	Method of Data Collection
Year 1	Styrofoam Ball Kit	In-lab	Anonymous paper surveys, before and after lab
Year 2	Acrylic Model Kit	In-lab	Anonymous paper surveys, before and after lab
Year 3	Acrylic Model Kit	Take-home, supported by in-lecture tutorial	Anonymized iClickers, before and after in-lecture tutorial

5.2.2 Participants:

The study involved three sample populations, “Year 1”, “Year 2”, and “Year 3”, consisting of approximately half of the students enrolled in Chemistry 101 at the University of Victoria in the fall semester of 2015, 2016, and 2017 respectively. The following table (Table 5.2) summarizes the number of participants in each group:

Table 5.2 Summary of participant data for each year of the study

	Number of participants		
	Asked to Participate	Participated (Pre-Exercise)	Participated (Post-Exercise)
Year 1	473	424	302
Year 2	520	362	278
Year 3	566	522	455

In Year 1 and Year 2, students from approximately half of the Chemistry 101 laboratory sections, chosen at random, were asked to participate in the study. In year 3, students from two of the three lecture sections were asked to participate in the study. As the study involved human participants, one of our primary concerns was to prevent or minimize potential risks of harm to the participants. The potential psychological and emotional risks associated with participation, identified through consultation with the Human Research Ethics Board at the University of Victoria, were minimized by ensuring that student participation in the study was voluntary. Additionally, the anonymity of the participants was protected to prevent any inducement effects from the existing power-over relationship between the principal investigators and the participants (see Appendix B for letter of information of implied consent).

5.2.3 Instruments

Representational Competence Assessment Surveys:

We created two similar versions of the survey, "Version A" and "Version B" (Figure 5.3 and Figure 5.4) each consisting of four questions designed to probe students' representational competence by testing a students' ability to visualize, mentally manipulate, and relate different representations. At the start of the laboratory session, half of the students were asked to complete "Version A" of the survey, and the other half were asked to complete "Version B". At the end of the laboratory session, those students who completed "Version A" were asked to complete "Version B", and the "Version B" students were asked to complete "Version A". Although the two versions of the survey were similar in nature, we alternated the versions in this manner to eliminate any potential bias if one of the survey versions was more difficult than the other.

1. Which of the following molecular fragments, when combined (by precisely overlapping the orange atoms) with the one shown on the right would generate an **octahedral** structure? (Circle one)

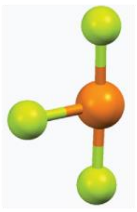

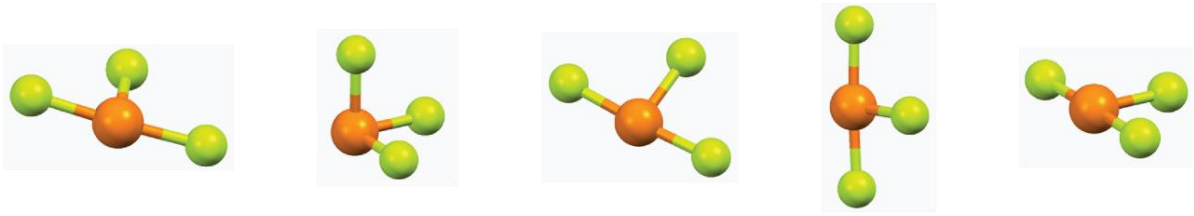

2. Of the following three-dimensional structures, which represents a molecular geometry that is different from the others? (Circle one)

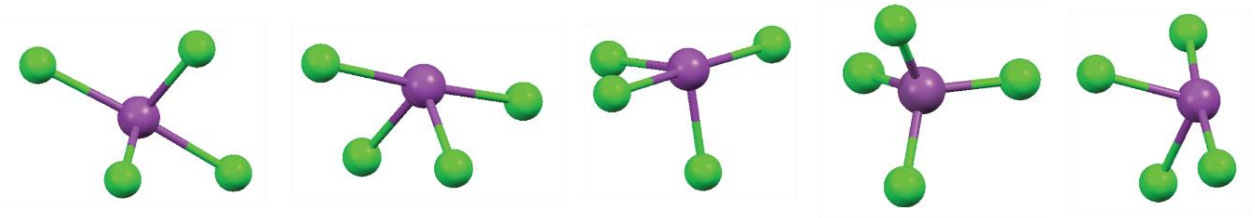

3. There are 3 different structures below, drawn with different dimensional projections. There are two structurally identical pairs and one unique structure. Circle the **unique** structure.

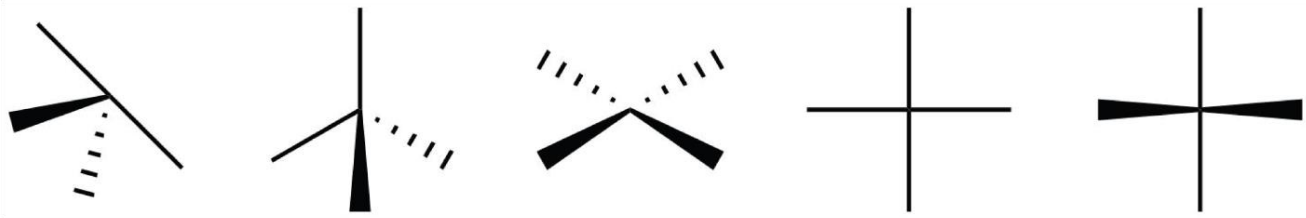

4. How many faces, **in total**, are there on the polyhedron shown below? (including the sides not shown)

a) 10 b) 12 c) 15 d) 20 e) 25

Figure 5.3 Representational Competence Assessment Survey (Version A).

1. Which of the following molecular fragments, when combined (by precisely overlapping the orange atoms) with the one shown on the right would generate a **trigonal bipyramidal** structure? (Circle one)

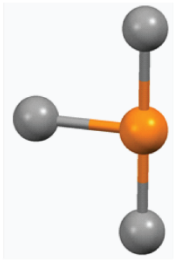

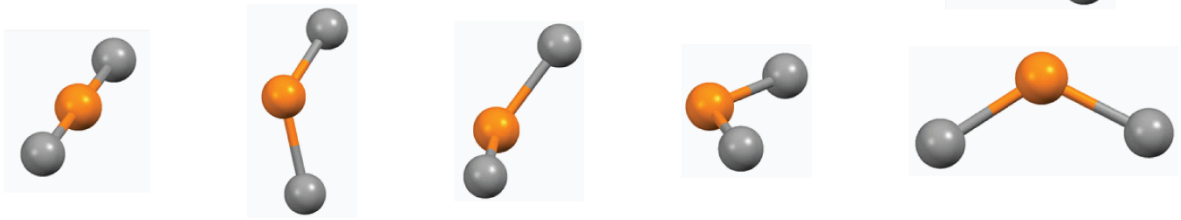

2. Of the following three-dimensional structures, which represents a molecular geometry that is different from the others? (Circle one)

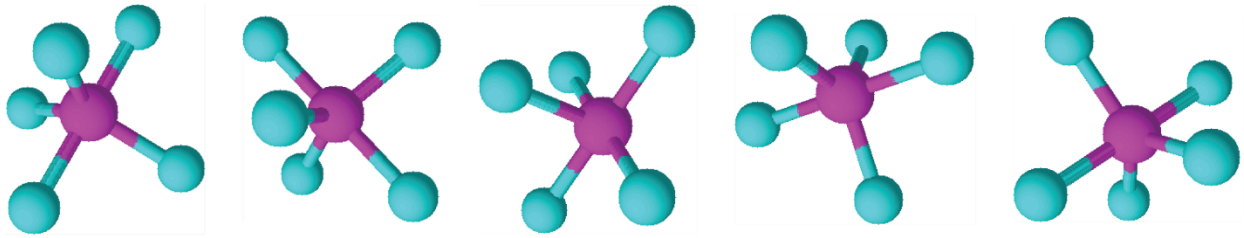

3. There are 3 different structures below, drawn with different dimensional projections. There are two structurally identical pairs and one unique structure. Circle the **unique** structure.

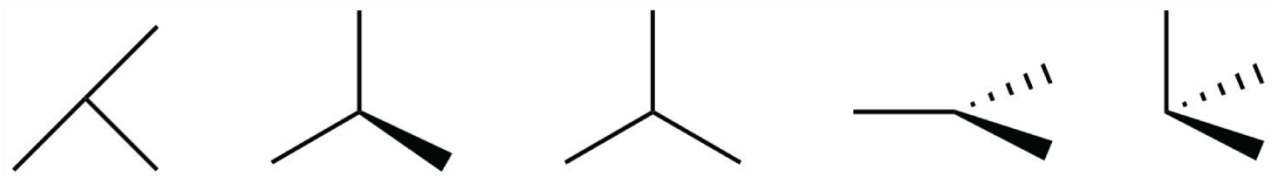

4. How many faces, **in total**, are there on the polyhedron shown below? (including sides not shown)

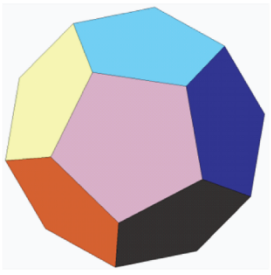

a) 8 b) 10 c) 12 d) 14 e) 16

Figure 5.4 Representational Competence Assessment Survey (Version B).

Using ‘Version A’ as an example, a more detailed description the questions and the skills required to solve them is as follows:

In question 1, students are given a molecular fragment and asked to identify the fragment for a set of answers that when superimposed would generate an octahedral molecule. This task requires students to sequentially take two images, visualize the representation generated when they are superimposed, and compare this to a mentally generated representation of octahedral molecular geometry to determine if they are the same.

For question 2, students are provided with five molecular representations - one tetrahedral and four ‘see-saw’ - and asked to identify which representation has a different molecular geometry from the rest. In order to correctly identify the different (i.e. tetrahedral) three-dimensional representations, students must mentally manipulate the representations and compare their spatial configurations.

Question 3 is similar to question 2; however, the students are given two-dimensional wedge-dash structures instead of three-dimensional molecular representations. This requires students to perform the additional task of mentally visualizing the three-dimensional structures before they can compare them.

In question 4, students are shown a polyhedron from a single perspective and asked to evaluate the total number of plane faces on the shape. This question was designed to provide insight into whether the effect of the exercise on representational competence abilities is domain-specific or domain-general, which remains a debated topic among researchers.[83]

Experience Questionnaires:

We also attempted to probe students' qualitative impressions of the exercise by asking them to indicate their degree of agreement - using a five-point Likert scale ranging from "strongly agree" to "strongly disagree" - with the following three statements during the post-exercise survey:

1. "I learned a lot about molecular shape in this laboratory"
2. "I enjoyed this laboratory class"
3. "I am likely to tell friends and family about my experience in this laboratory class"

Note: Questions were adjusted in Year 3, changing "laboratory class" for "take-home exercise"

5.2.4 Procedure

Year 1 & Year 2:

At the start of each selected laboratory section, the researcher reviewed the contents of the letter of information of implied consent with the students, outlining the details of the study and the nature of their participation. After the researcher left, the laboratory TA then administered the "Pre" surveys to the entire class as an individual closed-book activity. Students were given approximately 5 minutes to either (a) participate in the study through completion of the surveys, or (b) opt-out of the study and instead sitting quietly/doodling. The surveys were then collected by the TA, and students then went on to complete the laboratory exercise as outlined in the manual, using the model kit corresponding to the year. After the students completed the laboratory exercise, they were given the "Post" survey which they could choose to

do before leaving the lab. Considerations regarding the methodology of survey administration are discussed in section 5.3.3.

Year 3:

In Year 3, laboratory availability issues meant all students did the laboratory exercise instead as a take-home activity, with the material supported by an in-class lecture where the students brought along their model kits (see section 5.3 for further details). At the start of each lecture, the researcher reviewed the contents of the letter of information of implied consent with the students, outlining the details of the study and the nature of their participation. The surveys in Year 3 were administered to the class as a series of iClicker questions. To ensure the anonymity of the students was protected, students were asked to swap iClickers with another student before the data collection commenced. Students were then given approximately 1.25 minutes per question, which they could use to either answer the question, or sit quietly. The instructor, Dr. McIndoe, was not present at any point during the survey process, to protect the anonymity of the students and prevent any inducement effects from the existing power-over relationship. After the "Pre" survey was completed, the instructor then gave students an in-lecture tutorial on how to utilize these models in problem solving context. Following the completion of the exercise, the students were administered a "Post" survey using the same procedure.

5.2.5 Statistical Analysis of Data

Unless otherwise noted, statistical analysis of data was performed at the 95% confidence level (α=0.05), using Minitab statistical software. [84]

Incomplete survey data (i.e. surveys where a student left one or more question unanswered) were eliminated *a priori*, consistent with the students' right to withdraw participation at any time as

outline in the letter of information of implied consent. However, it is noted that if a student chose to participate fully in one survey but chose not to complete the other, we would not be able to detect or correct for this due to the anonymous nature of the study.

Assessment Data:

Data from the assessment portion of the surveys was treated as being approximately normal, consistent with Central Limit Theorem for large sample sizes, and was analyzed using standard parametric statistics. The assessment data was scored using a binary point system (1, correct; 0, incorrect) and summed to determine overall score out of a maximum 4 points. Within a given year, the sample means of the "Pre" and "Post" data sets were compared using a two-sample t-test and Cohen's d (pooled SD) was used to calculate and report effect size. Full set of descriptive statistics and for all 6 data sets ("Pre" and "Post" for Year 1, Year 2, and Year 3) can be found in Appendix B.

Questionnaire Data:

The responses from the questionnaire portion of the survey was converted into numerical scores using the point system outlined in Table 5.3.

Table 5.3. Conversion Table for Likert Data

Response	Strongly Agree	Agree	Neither Agree nor Disagree	Disagree	Strongly Disagree
Point Value	5	4	3	2	1

Data from the questionnaire portion of the surveys was analyzed using both parametric and non-parametric statistics. While non-parametric methods are more commonly used for ordinal data types, parametric testing is considered to be more rigorous than non-parametric, even when statistical assumptions such as normality are violated, and experts have concluded that it is acceptable for analyzing Likert scale data.[85] The response distribution for each question was qualitatively compared across all three years using graphical representations. The means were compared using two-sample t-tests, and the medians were compared using the Mann-Whitney U test (adjusted for ties). Full sets of descriptive statistics can be found in Appendix B.

5.3 Results and Discussion

5.3.1 Assessment Results

Analysis of the collective assessment data, summarized in Table 5.4, yielded mixed results and failed to reveal a clear trend in results between years. When comparing the average of the "Pre" and "Post" assessment scores, no statistically significant difference in overall score was observed ($p>0.05$) for either the Year 1 or the Year 2 groups. The lack of a significant improvement in performance in either Year 1 or Year 2 was somewhat puzzling, but perhaps partly a function of the observed reduced, and often perfunctory participation of the students in the "post-exercise" survey (see section 5.3 for further discussion)

Conversely, the before-and-after results from Year 3 showed a significant improvement in average score ($p < .001$, $d = 0.34$), with students scoring on average 9.7% ± 3.6% better on the "Post" assessments.

Table 5.4 Average scores, standard deviations, and improvement for pre- and post-exercise surveys

Sample	Pre-Exercise			Post-Exercise			Difference between Average Pre- and Post- Score, $\Delta\bar{x}$
	n_1	$\bar{x}_1$	s_1	n_2	$\bar{x}_2$	s_2	
Year 1	424	60.1%	0.9967	302	62.4%	1.084	Not Significant, $p > 0.05$
Year 2	362	59.0%	1.054	278	57.1%	1.138	Not Significant, $p > 0.05$
Year 3	522	50.0%	1.149	455	59.7%	1.142	+9.7% ±3.6%, $p < 0.001$

Comparing the Year 3 results for each question individually (Table 5.5), yields insight into the whether the effects of this intervention are domain-specific or not.

Table 5.5. Individual average pre- and post- scores for assessment question data (Year 3)

	Average Score (%)		
	Pre-Exercise	Post-Exercise	Difference between Average Pre- and Post- Score, Δx
Question 1	55.0	72.3	17.3 ± 5.9, $p<0.001$
Question 2	45.8	58.2	12.5 ± 6.3, $p<0.001$
Question 3	33.7	44.0	10.2 ± 6.1, $p<0.001$
Question 4	65.5	64.4	Not Significant, $p > 0.05$

The difference between average pre- and post- score was found to be surprisingly similar (in considering the significant overlap in confidence intervals between questions) for questions 1, 2, and 3, with improvement values of 17.3% ± 5.9%, 12.5% ± 6.3% and 10.2% ± 6.1%, respectively. Contrarily, the results from question 4 revealed no statistically significant difference in score after completing the exercise. This is of particular interest as it potentially indicates that the observed improvement in representational competence may be a domain-specific effect, rather than a general one. As the particular skills required to solve this problem, namely the ability to predict hidden properties of an object by extrapolating given visual

information, were not directly assessed in any of the other survey questions, further work is needed to substantiate this observation.

5.3.2 Questionnaire Results

In addition to examining the effect of the model kits on student representational competence skills, we attempted to gauge student opinion regarding the models and their effectiveness. The students were asked to indicate their degree of agreement, on a five-point scale as outlined in the methods section to the following three questions:

1. "I learned a lot about molecular shape in this laboratory"
2. "I enjoyed this laboratory class"
3. "I am likely to tell friends and family about my experience in this laboratory class"

The questionnaire results are summarized in Table 5.6, and detailed statistical analysis results for the comparison of the responses between each year are summarized in Appendix B.

Table 5.6 Descriptive Statistics for Questionnaire Data

		Question 1			Question 2			Question 3		
	N	Md	$\bar{x}$	CI	Md	$\bar{x}$	CI	Md	$\bar{x}$	CI
Year 1	303	4	3.67	0.109	4	3.13	0.130	4	3.25	0.135
Year 2	225	3	3.88	0.107	4	3.43	0.159	3	3.31	0.157
Year 3	475	3	3.28	0.091	3	3.13	0.107	3	2.71	0.112

N = sample size, Md = median, $\bar{x}$ = mean, CI = 95% confidence interval for mean ($\bar{x} \pm$ CI)

When each group of students (Year 1, 2, and 3) were asked if they felt they learned a lot about molecular shape during the laboratory/take-home exercise, the results indicate that students tended to agree, with positive responses ("agree" or "strongly agree") accounting for 70%, 78%,

and 51% respectively (Figure 5.5). The results revealed that the Year 2 group had the highest average response, indicating that a larger proportion of students felt that they learned a lot about molecular shape when the exercise utilized the acrylic model kits in an in-lab setting (Year 2) when compared to both Year 1 and Year 3. Most surprisingly, the Year 3 group had the lowest average response, indicating that a smaller proportion of students that felt that they learned a lot about molecular shape when the activity was run using the acrylic model kits as take-home exercise, relative to Year 1 and Year 2, even though the year 3 students were the only group to have achieved a significant improvement in average score during the assessment portion of the survey.

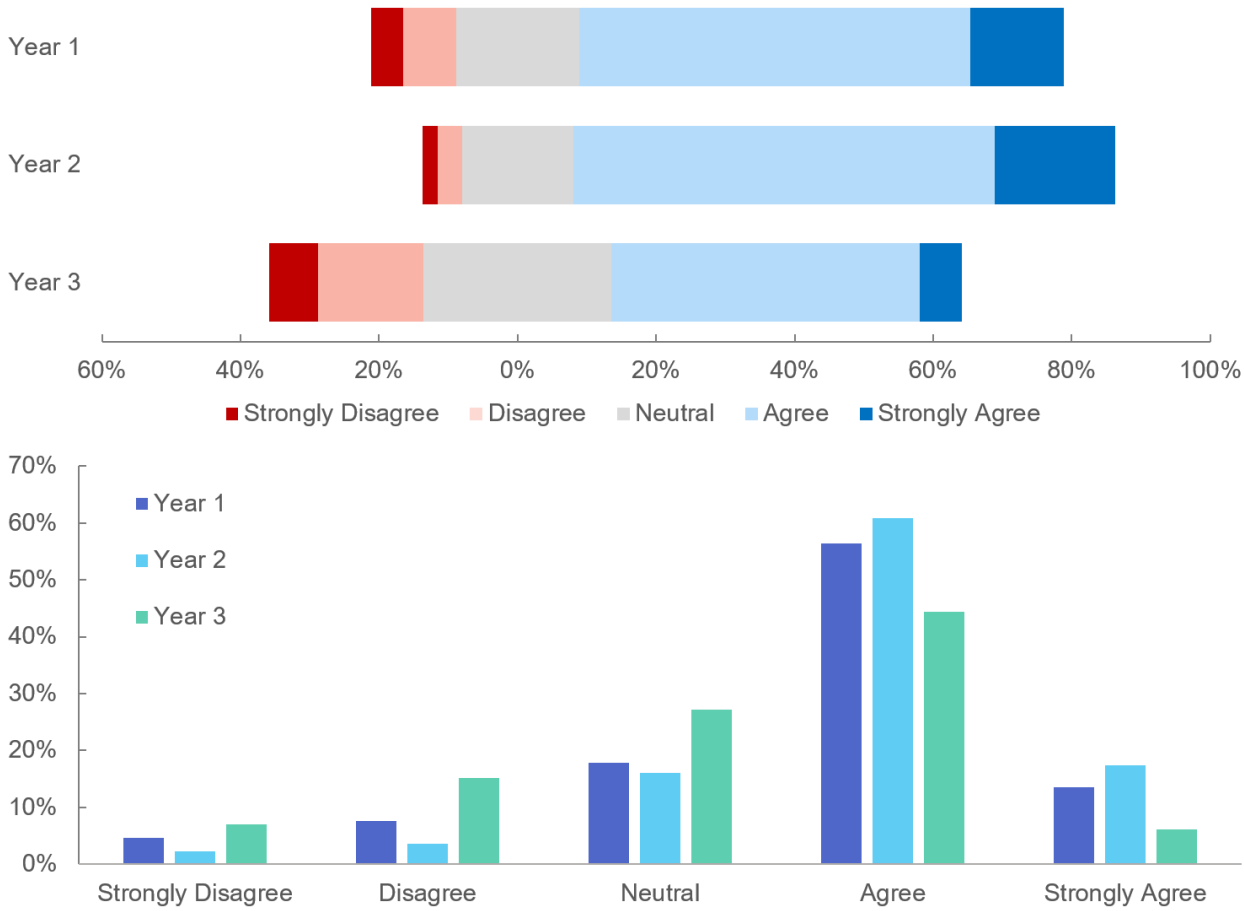

Figure 5.5 Response distribution for 'I learned a lot about molecular shape in this laboratory class/take-home exercise'

When the students were asked if they enjoyed the laboratory class/take-home exercise, the results were more neutral, with positive responses (“agree” or “strongly agree”) only accounting for only 42%, 56%, and 43% in Years 1, 2, and 3 respectively (Figure 5.6). Comparing the results revealed that the Year 2 group had the highest average response, indicating that a larger proportion of students enjoyed the activity when it utilized the acrylic model kits in an in-lab setting (Year 2) when compared to both Year 1 and Year 3. Contradictory to this result, there was no statistically significant difference found between the Year 1 and Year 3 results, potentially indicating that neither the method nor the activity type had any significant effect on student enjoyment.

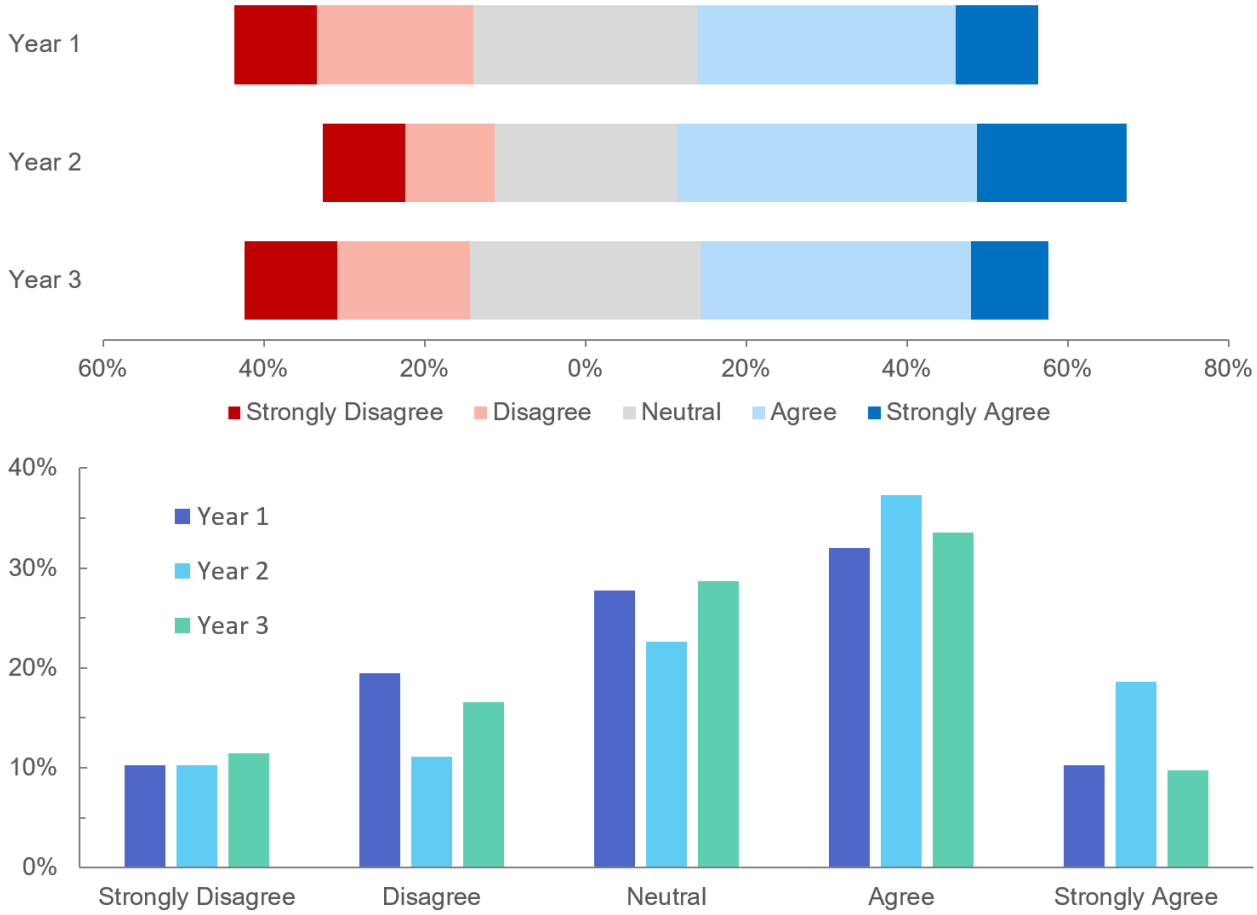

Figure 5.6. Response distribution for 'I enjoyed this laboratory class/take-home exercise'

When the students were asked if they were likely to tell friends and family about their experience in the laboratory class/take-home exercise, the results were mixed, with positive responses ("agree" or "strongly agree") only accounting for only 47%, 45%, and 29% in Years 1, 2, and 3 respectively (Figure 5.7). The Year 1 and Year 2 students tied for the highest average response, with no statistically significant difference found between the two groups. However, a significant decrease was observed when comparing both the responses of the Year 1 and Year 2 groups to those from Year 3, potentially indicating that a larger proportion of students were likely to share

their experiences when the activity was run as an in-laboratory exercise, relative to the take-home version.

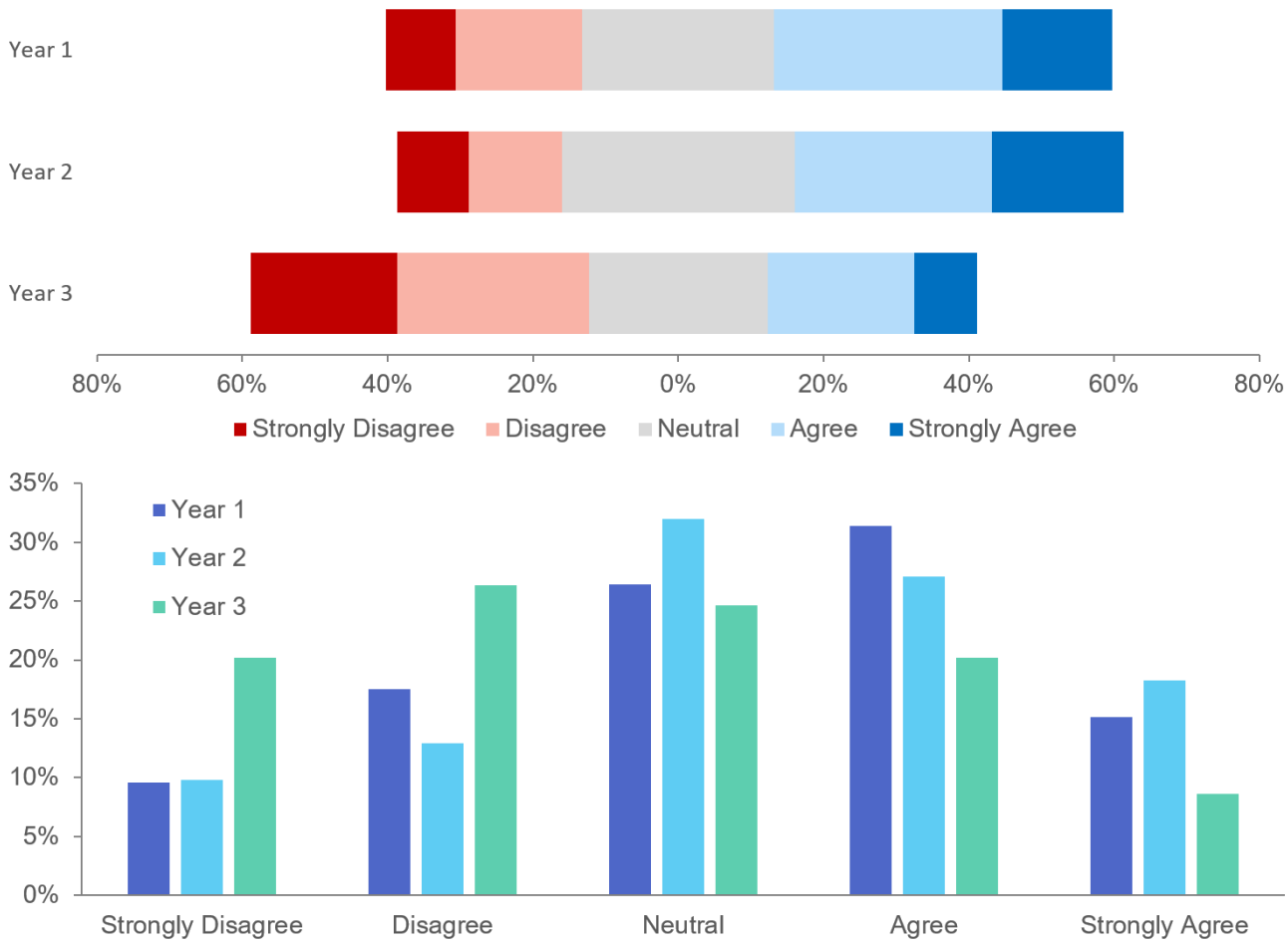

Figure 5.7 Response distribution for 'I am likely to tell friends and family about my experience in this laboratory class/take-home exercise'

5.3.3 Limitations and Considerations

Data Collection and Survey Administration

The deployment and assessment of these models occurred over a three-year period starting in the fall semester of 2015, which coincided with a major renovation of our first-year chemistry

laboratories. This disruption was problematic for us in fairly assessing the efficacy of our new approach relative to the original method, but it did also grant us considerable flexibility in delivering the exercise both in-lab and as a take-home assignment in lieu of a lab (in the term when the laboratory had limited availability due to renovations).

The surveys were originally designed to be administered by the section TA, as an individual closed-book activity to the entire laboratory section simultaneously, with approximately 5 minutes of laboratory time dedicated to the study at the start and end of the session. Students then had the option of either using this time to: (a) participate in the study through completion of the surveys, or (b) opting-out of the study and instead sitting quietly/doodling. The study was designed this way so that students who chose to opt-out couldn't continue working or socializing, resulting in the participants feeling disadvantaged.

During the Year 1 study, this method worked well for the administration of the "pre-exercise" surveys; however, we found that this method was not practically feasible for the "post-exercise" survey. The time students took to complete the laboratory exercise varied greatly, making simultaneous completion of the surveys unrealistic, and we were forced to adjust accordingly. Instead, as students left the lab, they could choose whether or not to complete the "post-exercise" survey. In Year 2, for sake of consistency, we chose to keep all aspects of the study identical to that of Year 1, changing only the model kits used.

While we believed (*a priori*) that this change in method would have minimal effects on the study, we observed (*a posteriori*) that this was likely not the case and that the reliability of the results for the Year 1 and Year 2 groups may have been affected. Instead, as a result of the voluntary nature of the study, we observed that the participation in the "post-exercise" survey was not only reduced but often perfunctory. We found students were keen to go home or to their

next class, which resulted in a large number of students either choosing not to do the survey or rushing through it and not devoting significant thought to their answers. As a result of this, the data obtained during the "post-exercise" survey of Year 1 and Year 2 likely contains systematic bias, as proper randomization of the sample was not achieved, and should be considered when interpreting the validity of the study results.

We determined that a better method of surveying was necessary, where students didn't feel disadvantaged by choosing to participate in the survey, and an opportunity arose to do so in Year 3. Laboratory availability issues meant all students did the laboratory exercise instead as a take-home activity, with the material supported by an in-class lecture where the students brought along their model kits. This allowed us to administer the surveys simultaneously in a controlled way, using anonymized iClickers with fixed time limits. As a result, we felt that we were better able to acquire reliable data, without the aforementioned sampling bias for both the "pre-exercise" and "post-exercise" surveys and therefore this method is recommended for use in future work.

It is noted that while the 2017 Chemistry 101 course had three sections taught by two different instructors, out of convenience only students in the sections taught by Dr. McIndoe were asked to participate, introducing a source of selection bias which may affect the accuracy of the Year 3 results. Future work should include either the entire chemistry 101 population or employ a rigorous random sampling technique to eliminate this source of bias.

Survey Design

As the study involved a large number of participants, the assessment portion of the surveys was designed using closed-style questions, as they allow for simplified collation and analysis the data.

Assessment Questions

For the assessment portion of the survey, the multiple-choice format used - consisting of questions with binary outcomes (i.e. correct or incorrect answer, no partial marks) - allows for scoring of the data to remain objective. Because of this, multiple choice questions are often considered to have a high degree of reliability,[86] which is particularly important when deriving conclusions through comparison of pre-test/post-test data.[87] While this style of question was determined to be the ideal format for the surveys of this study, multiple choice questions do have inherent disadvantages – primarily ambiguity in the interpretation of the question by the examinee and blind guessing - that also play a role in the consistency and reliability of the results.[88] A number of design-dependent factors influence the reliability and validity of multiple choice testing, such as (but not limited to): the number of questions asked, question difficulty, question content, and the number and quality of distractors (incorrect answers).[89] As a formal evaluation of the survey questions was not done for this study, it is difficult to provide meaningful commentary on the reliability and validity of the questions used. Future work should include a series of pilot studies (ie. asking small groups of participants to indicate how they interpret the questions being asked) to assess and optimize the survey questions, as well as a rigorous statistical evaluation regarding the reliability and validity of questions and results.

Questionnaire Questions

The questionnaire portion of the surveys was designed using five-point Likert-scale (or rating-scale) questions, which allows degrees of opinion to be measured. Likert-scales are considered to be the most reliable tool for assessing attitudes;[90,91] however, the structuring of the questions and the interpretation by the participants can potentially have a large impact on the results.[85,92] It was

determined, retrospectively, that there were potential issues with the phrasing of questions 2 and 3 in this portion of the survey, which should be considered when interpreting the results.

While question 2, “I enjoyed this laboratory class”, was intended to measure and compare student enjoyment relative to the type of model used, the students response could potentially also be a reflection of their enjoyment of: the actual laboratory exercise for which the models are used, their experience in their laboratory section (including opinions of TA and/or peers), the laboratory course as a whole, or the take-home nature of the Year 3 version. In future, this question should be rephrased to specify enjoyment relative to the type of model used.

Question 3 was designed “I am likely to tell friends and family about my experience in this laboratory class” with the notion that students would be likely share a positive in-lab experience with their family and friends; however, it fails to consider that if the students had a particularly poor experience, they may be equally likely to share this with others. In addition, the student’s response may be affected by the personality of the student as well as the nature of the relationship they have with their friends and family. Based on these factors, this question should be heavily revised to specify whether students would be likely to reflect upon their experiences using the molecular models once they have finished the activity, and whether they would be likely to share their experience of using the model kits with others.

5.4 Conclusions and Future Work

Overall, students responded positively to the permanent provision of three dimensional models of the molecular shapes taught in first year. The laser-cut acrylic pieces used were easy to produce and inexpensive enough that they could be given to the students to take home after class,

providing them with an enduring reminder of the spatial concepts they were taught in the class and laboratory. Initial results from the assessment of the acrylic model kits support the conclusion that the laser-cut acrylic model kits improve domain-specific representational competence and understanding of molecular geometry when accompanied by explicit instructional support; however, additional work is required to fully substantiate this observation. Repeating the study with the proposed improvements implemented would allow for a more complete assessment of the model kits to be conducted. In addition, more reliable control data is required to rigorously evaluate the efficacy of the acrylic models relative to the Styrofoam version. Future work should also include conducting a semester-long study to assess the effect of the model kits on overall performance on course material, which could be achieved by assigning different model kits to each section of the course and comparing overall student achievement, allowing for correlation between performance and type of model kit used.

Bibliography

(1) Thomson, J. J. Bakerian Lecture: Rays of Positive Electricity. *Proc. R. Soc. A Math. Phys. Eng. Sci.* **1913**, *89* (607), 1–20.

(2) Aston, F. W. A Positive Ray Spectrograph. *Philos. Mag. Ser. 6* **1919**, *38* (228), 707–714.

(3) Maccoll, A. Mass Spectrometry, Historical Perspective. In *Encyclopedia of Spectroscopy and Spectrometry*; Lindon, J. C., Ed.; Elsevier: Oxford, 2010; pp 1452–1458.

(4) Tang, K.; Page, J. S.; Kelly, R. T.; Marginean, I. Electrospray Ionization in Mass Spectrometry. In *Encyclopedia of Spectroscopy and Spectrometry*; Elsevier, 2010; pp 467–474.

(5) Henderson, W.; McIndoe, J. S. Ionisation Techniques. In *Mass Spectrometry of Inorganic, Coordination and Organometallic Compounds*; John Wiley & Sons, Ltd: Chichester, UK, 2005; pp 47–105.

(6) Henderson, W.; Mcindoe, J. S.; Nicholson, B. K.; Dyson, P. J. Electrospray Mass Spectrometry of Metal Carbonyl Complexes. *J. Chem. Soc. Dalt. Trans* **1998**, 519–525.

(7) Ho, C. S.; Lam, C. W. K.; Chan, M. H. M.; Cheung, R. C. K.; Law, L. K.; Lit, L. C. W.; Ng, K. F.; Suen, M. W. M.; Tai, H. L. Electrospray Ionisation Mass Spectrometry: Principles and Clinical Applications. *Clin. Biochem. Rev.* **2003**, *24* (1), 3–12.

(8) Janusson, E.; Hesketh, A. V.; Bamford, K. L.; Hatlelid, K.; Higgins, R.; McIndoe, J. S. Spatial Effects on Electrospray Ionization Response. *Int. J. Mass Spectrom.* **2015**, *388*, 1–8.

(9) Pramanik, B. N.; Ganguly, A. K.; Gross, M. L. *Applied Electrospray Mass Spectrometry*; Marcel Dekker, 2002.

(10) Zhang, J.-T.; Wang, H.-Y.; Zhu, W.; Cai, T.-T.; Guo, Y.-L. Solvent-Assisted Electrospray Ionization for Direct Analysis of Various Compounds (Complex) from Low/Nonpolar Solvents and Eluents. *Anal. Chem.* **2014**, *86* (18), 8937–8942.

(11) Henderson, W.; McIndoe, J. S. Mass Analysers. In *Mass Spectrometry of Inorganic, Coordination and Organometallic Compounds*; John Wiley & Sons, Ltd: Chichester, UK, 2005; pp 23–46.

(12) Skoog, D. A.; Holler, F. J.; Crouch, S. R. *Principles of Instrumental Analysis*; Cengage Learning, 2017.

(13) Vikse, K. L.; Ahmadi, Z.; Luo, J.; van der Wal, N.; Daze, K.; Taylor, N.; McIndoe, J. S. Pressurized Sample Infusion: An Easily Calibrated, Low Volume Pumping System for ESI-MS Analysis of Reactions. *Int. J. Mass Spectrom.* **2012**, *323–324*, 8–13.

(14) Yunker, L. P. E.; Stoddard, R. L.; McIndoe, J. S. Practical Approaches to the ESI-MS Analysis of Catalytic Reactions. *J. Mass Spectrom.* **2014**, *49* (1), 1–8.

(15) Ahmadi, Z.; Yunker, L. P. E.; Oliver, A. G.; McIndoe, J. S.; Haaren, R. J. van; Eerden, A. M. J. van der; Leeuwen, P. W. N. M. van; Koningsberger, D. C. Mechanistic Features of the Copper-Free Sonogashira Reaction from ESI-MS. *Dalt. Trans.* **2015**, *44* (47), 20367–20375.

(16) Hatanaka, Y.; Hiyama, T. Cross-Coupling of Organosilanes with Organic Halides Mediated by a Palladium Catalyst and Tris(diethylamino)sulfonium Difluorotrimethylsilicate. *J. Org. Chem.* **1988**, *53* (4), 918–920.

(17) Hiyama, T.; Hatanaka, Y. Palladium-Catalyzed Cross-Coupling Reaction of Organometalloids through Activation with Fluoride Ion. *Pure Appl. Chem.* **1994**, *66* (7).

(18) Hiyama, T. Organosilicon Compounds. In *Cross-Coupling Reactions*; Miyaura, N., Ed.; Springer-Verlag Berlin Heidelberg, 2002; pp 61–85.

(19) Sore, H. F.; Galloway, W. R. J. D.; Spring, D. R. Palladium-Catalysed Cross-Coupling of Organosilicon Reagents. *Chem. Soc. Rev.* **2012**, *41* (5), 1845–1866.

(20) Hatanaka, Y.; Goda, K.; Okahara, Y.; Hiyama, T. Highly Selective Cross-Coupling Reactions of Aryl(halo)silanes with Aryl Halides: A General and Practical Route to Functionalized Biaryls. *Tetrahedron* **1994**, *50* (28), 8301–8316.

(21) Hatanaka, Y.; Hiyama, T. Highly Selective Cross-Coupling Reactions of Organosilicon Compounds Mediated by Fluoride Ion and a Palladium Catalyst. *Synlett* **1991**, *1991* (12), 845–853.

(22) Amatore, C.; Grimaud, L.; Le Duc, G.; Jutand, A. Three Roles for the Fluoride Ion in Palladium-Catalyzed Hiyama Reactions: Transmetalation of [ArPdFL $_2$] by Ar′Si(OR) $_3$. *Angew. Chemie Int. Ed.* **2014**, *53* (27), 6982–6985.

(23) Sugiyama, A.; Ohnishi, Y.; Nakaoka, M.; Nakao, Y.; Sato, H.; Sakaki, S.; Nakao, Y.; Hiyama, T. Why Does Fluoride Anion Accelerate Transmetalation between Vinylsilane and palladium(II)-Vinyl Complex? Theoretical Study. *J. Am. Chem. Soc.* **2008**, *130* (39), 12975–12985.

(24) Denmark, S. E.; Sweis, R. F.; Wehrli, D. Fluoride-Promoted Cross-Coupling Reactions of Alkenylsilanols. Elucidation of the Mechanism through Spectroscopic and Kinetic Analysis. *J. Am. Chem. Soc.* **2004**, *126* (15), 4865–4875.

(25) Dean, N. L. Mechanistic Investigation of the Hiyama Cross Coupling Reaction, Undergraduate Thesis (B.Sc.), University of Victoria, 2015.

(26) Díaz-Torres, R.; Alvarez, S. Coordinating Ability of Anions and Solvents towards Transition Metals and Lanthanides. *Dalt. Trans.* **2011**, *40* (40), 10742.

(27) Szabó, P. T.; Kele, Z. Electrospray Mass Spectrometry of Hydrophobic Compounds Using Dimethyl Sulfoxide and Dimethylformamide as Solvents. *Rapid Commun. Mass Spectrom.* **2001**, *15* (24), 2415–2419.

(28) Precision Seal Septa | Sigma-Aldrich http://www.sigmaaldrich.com/labware/products/precision-seal.html (accessed May 1, 2017).

(29) Patiny, L.; Borel, A. ChemCalc: A Building Block for Tomorrow's Chemical Infrastructure. *J. Chem. Inf. Model.* **2013**, *53* (5), 1223–1228.

(30) Poh, B. T.; Te, C. S. Cure Index and Activation Energy of Vulcanization of Natural Rubber and Epoxidized Natural Rubber Vulcanized in the Presence of Antioxidants. *J. Appl. Polym. Sci.* **2000**, *77* (14), 3234–3238.

(31) Sharma, R. K.; Fry, J. L. Instability of Anhydrous Tetra-N-Alkylammonium Fluorides. *J. Org. Chem.* **1983**, *48* (12), 2112–2114.

(32) Luo, J.; Oliver, A. G.; Scott McIndoe, J. A Detailed Kinetic Analysis of Rhodium-Catalyzed Alkyne Hydrogenation. *Dalt. Trans.* **2013**, *42* (31), 11312.

(33) Luo, J.; Wu, Y.; Zijlstra, H. S.; Harrington, D. A.; McIndoe, J. S. Mass Transfer and Convection Effects in Small-Scale Catalytic Hydrogenation. *Catal. Sci. Technol.* **2017**, *7* (12), 2609–2615.

(34) Luo, J.; Theron, R.; Sewell, L. J.; Hooper, T. N.; Weller, A. S.; Oliver, A. G.; McIndoe, J. S. Rhodium-Catalyzed Selective Partial Hydrogenation of Alkynes. *Organometallics* **2015**, *34* (12), 3021–3028.

(35) Marsella, J. A. Dimethylformamide. In *Kirk-Othmer Encyclopedia of Chemical Technology*; John Wiley & Sons, Inc.: Hoboken, NJ, USA, 2000.

(36) Sun, H.; DiMagno, S. G. Anhydrous Tetrabutylammonium Fluoride. *J. Am. Chem. Soc.* **2005**, *127* (7), 2050–2051.

(37) Biddle, M. M.; Reich, H. J. Studies on the Reactive Species in Fluoride-Mediated Carbon-Carbon Bond-Forming Reactions: Carbanion Formation by Desilylation with Fluoride and Enolates. *J. Org. Chem.* **2006**, *71* (11), 4031–4039.

(38) Shenderovich, I. G.; Smirnov, S. N.; Denisov, G. S.; Gindin, V. A.; Golubev, N. S.; Dunger, A.; Reibke, R.; Kirpekar, S.; Malkina, O. L.; Limbach, H.-H. Nuclear Magnetic Resonance of Hydrogen Bonded Clusters between F− and (HF)n: Experiment and Theory. *Berichte der Bunsengesellschaft für Phys. Chemie* **1998**, *102* (3), 422–428.

(39) Engelhardt, G. Fluorine-19 NMR and Ir Spectroscopic Study of Organofluorosilanes and Organofluorogermanes. *Zeitschrift für Chemie* **1970**, *10* (7), 266–267.

(40) Penso, M.; Albanese, D.; Landini, D.; Lupi, V. Biaryl Formation: Palladium Catalyzed Cross-Coupling Reactions between Hypervalent Silicon Reagents and Aryl Halides. *J. Mol. Catal. A Chem.* **2003**, *204–205*, 177–185.

(41) Damrauer, R.; Danahey, S. E. Preparation and NMR Studies of Pentacoordinated Silicon

Anions. *Organometallics* **1986**, *5* (7), 1490–1494.

(42) Marat, R. K.; Janzen, A. F. Fluorine Exchange between Four-, Five-, and Six-Coordinate Silicon Compounds. *Can. J. Chem.* **1977**, *55* (22), 3845–3849.

(43) Reich, H. J. Fluorine NMR Data http://chem.wisc.edu/areas/reich/handouts/nmr/f-data.htm (accessed Mar 27, 2018).

(44) Dean, N. L.; Ewan, C.; McIndoe, J. S. Applying Hand-Held 3D Printing Technology to the Teaching of VSEPR Theory. *J. Chem. Educ.* **2016**, *93* (9), 1660–1662.

(45) Zare, R. N. Visualizing Chemistry. *J. Chem. Educ.* **2002**, *79* (11), 1290.

(46) Stull, A. T.; Hegarty, M. Model Manipulation and Learning: Fostering Representational Competence with Virtual and Concrete Models. *J. Educ. Psychol.* **2016**, *108* (4), 509–527.

(47) Sim, J. H.; Daniel, E. G. S. Representational Competence in Chemistry: A Comparison between Students with Different Levels of Understanding of Basic Chemical Concepts and Chemical Representations. *Cogent Educ.* **2014**, *1* (1), 2–17.

(48) Khine, M. S. Spatial Cognition: Key to STEM Success. In *Visual-spatial Ability in STEM Education*; Springer International Publishing: Cham, 2017; pp 3–8.

(49) Kozma, R. B.; Russell, J. Multimedia and Understanding: Expert and Novice Responses to Different Representations of Chemical Phenomena. *J. Res. Sci. Teach.* **1997**, *34* (9), 949–968.

(50) Stieff, M.; Scopelitis, S.; Lira, M. E.; Desutter, D. Improving Representational Competence with Concrete Models. *Sci. Educ.* **2016**, *100* (2), 344–363.

(51) Russell, J.; Kozma, R. Assessing Learning from the Use of Multimedia Chemical Visualiztion Software. In *Visualization in Science Education*; Springer Netherlands: Dordrecht, 2005; pp 299–332.

(52) Justi, R.; Gilbert, J. The Role of Analog Models in the Understanging of the Nature of Models in Chemistry. In *Metaphor and Analogy in Science Education*; Springer-Verlag: Berlin/Heidelberg, 2006; pp 119–130.

(53) Treagust, D. F.; Chittleborough, G. Chemistry: A Matter of Understanding Representations. In *Subject-specific instructional methods and activities (Advances in Research on Teaching, Volume 8)*; Emerald Group Publishing Limited, 2001; pp 239–267.

(54) Coll, R. K.; France, B.; Taylor, I. The Role of Models/and Analogies in Science Education: Implications from Research. *Int. J. Sci. Educ.* **2005**, *27* (2), 183–198.

(55) Cooper, M. M.; Underwood, S. M.; Hilley, C. Z.; Klymkowsky, M. W. Development and Assessment of a Molecular Structure and Properties Learning Progression. *J. Chem. Educ.* **2012**, *89* (11), 1351–1357.

(56) Grove, N. P.; Cooper, M. M.; Rush, K. M. Decorating with Arrows: Toward the Development of Representational Competence in Organic Chemistry. *J. Chem. Educ.* **2012**, *89* (7), 844–849.

(57) Carlisle, D.; Tyson, J.; Nieswandt, M. Fostering Spatial Skill Acquisition by General Chemistry Students. *Chem. Educ. Res. Pract.* **2015**, *16* (3), 478–517.

(58) Shah, P.; Miyake, A. The Separability of Working Memory Resources for Spatial Thinking and Language Processing: An Individual Differences Approach. *J. Exp. Psychol. Gen.* **1996**, *125* (1), 4–27.

(59) Stull, A. T.; Hegarty, M.; Dixon, B.; Stieff, M. Representational Translation With Concrete Models in Organic Chemistry. *Cogn. Instr.* **2012**, *30* (4), 404–434.

(60) Dragojlovic, V. Improving a Lecture-Size Molecular Model Set by Repurposing Used Whiteboard Markers. *J. Chem. Educ.* **2015**, *92* (8), 1412–1414.

(61) Sunderland, D. P. Studying Crystal Structures through the Use of Solid-State Model Kits. *J. Chem. Educ.* **2014**, *91* (3), 432–436.

(62) Kundell, F. A. A Simple VSEPR Demonstration. *J. Chem. Educ.* **1992**, *69* (4), 277.

(63) Shaw, C. F.; Shaw, B. A. A Magnetic Two-Dimensional Analogue of VSEPR. *J. Chem. Educ.* **1991**, *68* (10), 861.

(64) Hervas, M.; Silverman, L. P. A Magnetic Illustration of the VSEPR Theory. *J. Chem. Educ.* **1991**, *68* (10), 861.

(65) Lechner, J. H. The VSEPR Tree: A Hands-On Activity for Learning Molecular Geometry. *J. Chem. Educ.* **1994**, *71* (12), 1021.

(66) Kemp, K. C. A Novel, Simple, and Inexpensive Model for Teaching VSEPR Theory. *J. Chem. Educ.* **1988**, *65* (3), 222.

(67) Meloan, C. E. A Visual Aid to Demonstrate the VSEPR Theory. *J. Chem. Educ.* **1980**, *57* (9), 668.

(68) Becker, R. Coffee-Stirrer Structures. *J. Chem. Educ.* **1991**, *68* (6), 459.

(69) Donaghy, K. J.; Saxton, K. J. Connecting Geometry and Chemistry: A Three-Step Approach to Three-Dimensional Thinking. *J. Chem. Educ.* **2012**, *89* (7), 917–920.

(70) Scalfani, V. F.; Vaid, T. P. 3D Printed Molecules and Extended Solid Models for Teaching Symmetry and Point Groups. *J. Chem. Educ.* **2014**, *91* (8), 1174–1180.

(71) Meyer, S. C. 3D Printing of Protein Models in an Undergraduate Laboratory: Leucine Zippers. *J. Chem. Educ.* **2015**, 2120–2125.

(72) Rodenbough, P. P.; Vanti, W. B.; Chan, S.-W. 3D-Printing Crystallographic Unit Cells for

Learning Materials Science and Engineering. *J. Chem. Educ.* **2015**, *92* (11), 1960–1962.

(73) Griffith, K. M.; Cataldo, R. de; Fogarty, K. H. Do-It-Yourself: 3D Models of Hydrogenic Orbitals through 3D Printing. *J. Chem. Educ.* **2016**, *93* (9), 1586–1590.

(74) Smiar, K.; Mendez, J. D. Creating and Using Interactive, 3D-Printed Models to Improve Student Comprehension of the Bohr Model of the Atom, Bond Polarity, and Hybridization. *J. Chem. Educ.* **2016**, *93* (9), 1591–1594.

(75) Kaliakin, D. S.; Zaari, R. R.; Varganov, S. A. 3D Printed Potential and Free Energy Surfaces for Teaching Fundamental Concepts in Physical Chemistry. *J. Chem. Educ.* **2015**, *92* (12), 2106–2112.

(76) Carroll, F. A.; Blauch, D. N. 3D Printing of Molecular Models with Calculated Geometries and P Orbital Isosurfaces. *J. Chem. Educ.* **2017**, *94* (7), 886–891.

(77) Penny, M. R.; Cao, Z. J.; Patel, B.; Sil dos Santos, B.; Asquith, C. R. M.; Szulc, B. R.; Rao, Z. X.; Muwaffak, Z.; Malkinson, J. P.; Hilton, S. T. Three-Dimensional Printing of a Scalable Molecular Model and Orbital Kit for Organic Chemistry Teaching and Learning. *J. Chem. Educ.* **2017**, *94* (9), 1265–1271.

(78) Blauch, D. N.; Carroll, F. A. 3D Printers Can Provide an Added Dimension for Teaching Structure–Energy Relationships. *J. Chem. Educ.* **2014**, *91* (8), 1254–1256.

(79) Jones, O. A. H.; Spencer, M. J. S. A Simplified Method for the 3D Printing of Molecular Models for Chemical Education. *J. Chem. Educ.* **2018**, *95* (1), 88–96.

(80) Higman, C. S.; Situ, H.; Blacklin, P.; Hein, J. E. Hands-On Data Analysis: Using 3D Printing To Visualize Reaction Progress Surfaces. *J. Chem. Educ.* **2017**, *94* (9), 1367–1371.

(81) Bharti, N.; Singh, S. Three-Dimensional (3D) Printers in Libraries: Perspective and Preliminary Safety Analysis. *J. Chem. Educ.* **2017**, *94* (7), 879–885.

(82) Reimer, M.; Yunker, L. P. E.; Brant, M.; McIndoe, J. S. *Chemistry 101 Laboratory Manual*; Briggs, S., Ed.; University of Victoria: Victoria, 2015.

(83) diSessa, A. A.; Sherin, B. L. Meta-Representation: An Introduction. *J. Math. Behav.* **2000**, *19* (4), 385–398.

(84) Minitab Statistical Software. Minitab Inc.: State College, PA 2017.

(85) Jamieson, S. Likert Scales: How to (Ab)use Them. *Med. Educ.* **2004**, *38* (12), 1217–1218.

(86) Haladyna, T. M.; Rodriguez, M. C. *Developing and Validating Test Items*, 3rd ed.; Lawrence Erlbaum Associates, 2013.

(87) Polgar, Stephen. Thomas, S. *Introduction to Research in the Health Sciences*, 6th ed.;

Churchill Livingstone, 2000.

(88) Downing, S. M. Reliability: On the Reproducibility of Assessment Data. *Med. Educ.* **2004**, *38* (9), 1006–1012.

(89) Considine, J.; Botti, M.; Thomas, S. Design, Format, Validity and Reliability of Multiple Choice Questions for Use in Nursing Research and Education. *Collegian.* **2005**, *12* (1), 19–24.

(90) Tittle, C. R.; Hill, R. J. Attitude Measurement and Prediction of Behavior: An Evaluation of Conditions and Measurement Techniques. *Sociometry* **1967**, *30* (2), 199.

(91) Moors, G. Exploring the Effect of a Middle Response Category on Response Style in Attitude Measurement. *Qual. Quant.* **2008**, *42* (6), 779–794.

(92) Dolnicar, S. Asking Good Survey Questions. *J. Travel Res.* **2013**, *52* (5), 551–574.

Appendix A (Mechanistic Investigation of the Fluoride-mediated Rearrangement of Phenylfluorosilanes in the Hiyama Cross-Coupling Reaction by ESI-MS)

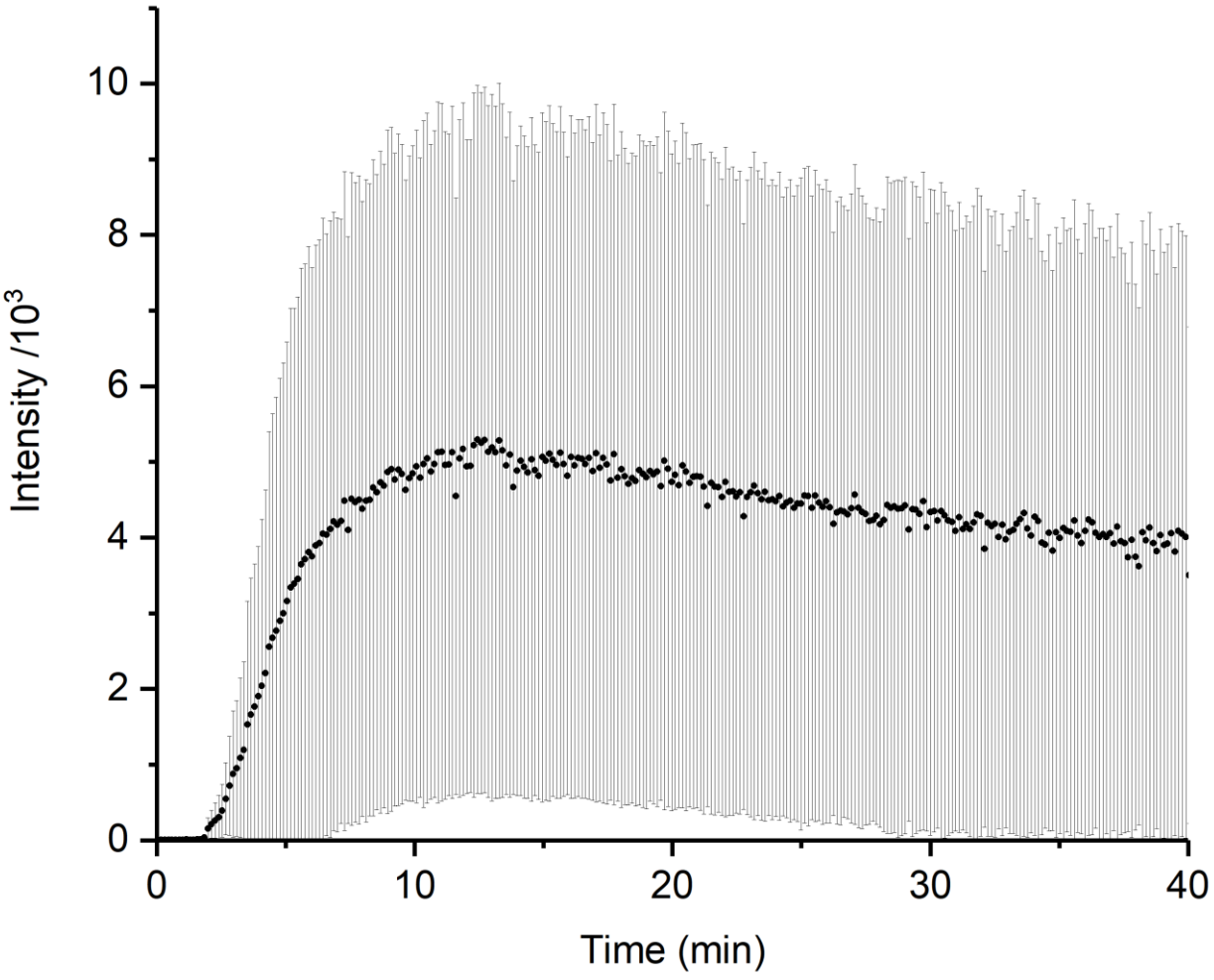

Figure A.1 Error bar plot for the intensity of $[Ph_2SiF_3]^-$ (*m/z* 239) over time, data averaged from three replicates.

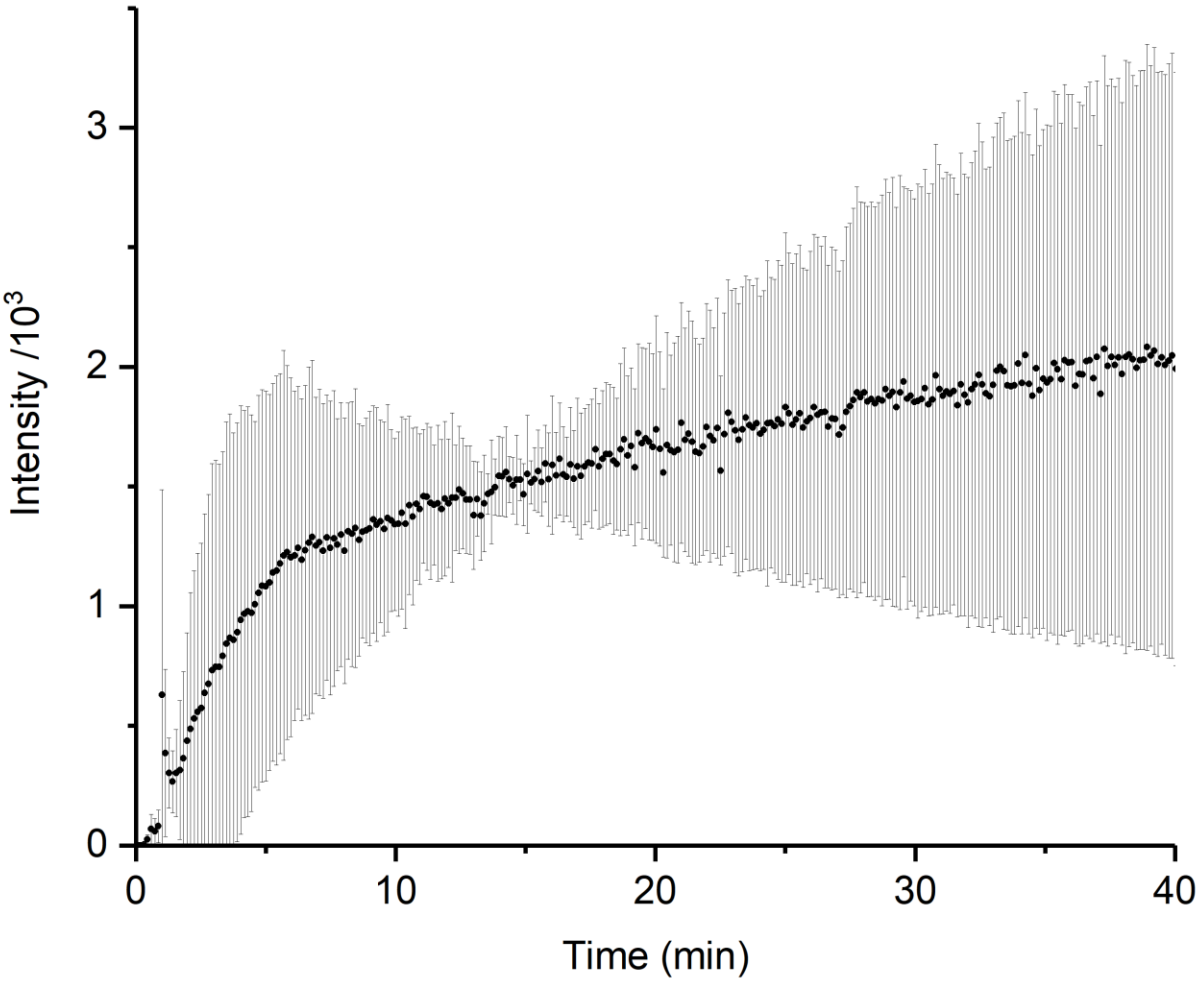

Figure A.2 Error bar plot for the intensity of $[PhSiF_4]^-$ (*m/z* 181) over time, data averaged from three replicates.

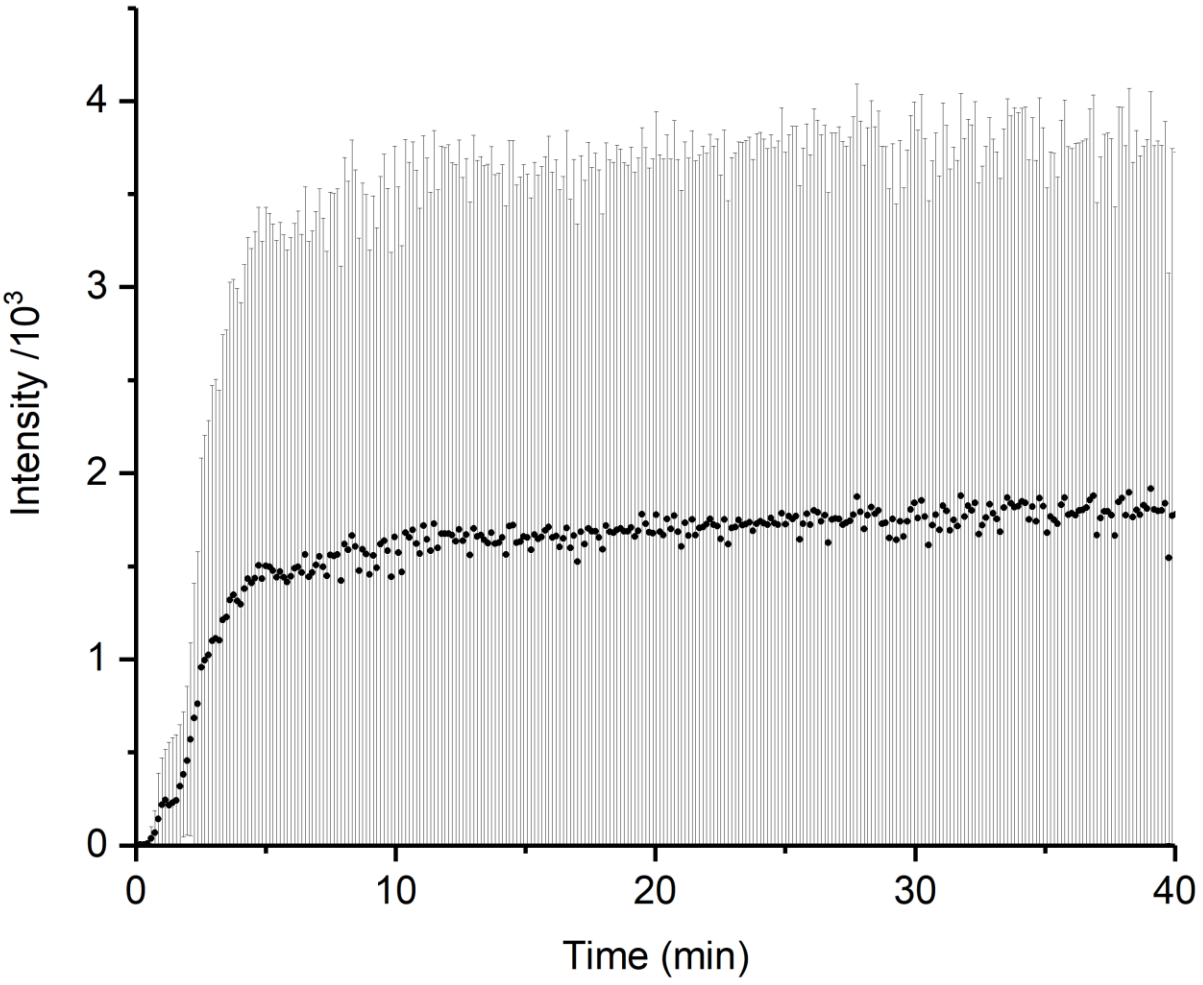

Figure A.3 Error bar plot for the intensity of $[SiF_5]^-$ (*m/z* 123) over time, data averaged from three replicates.

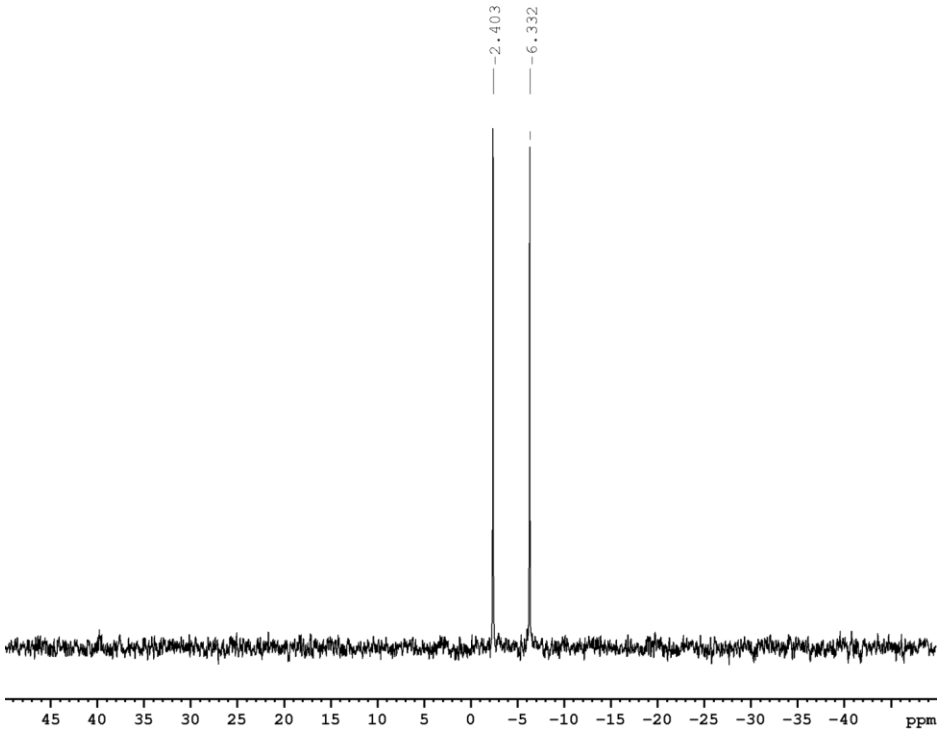

Figure A.4 ^{29}Si NMR spectrum of Ph_3SiF (d_6-DMSO, 360MHz)

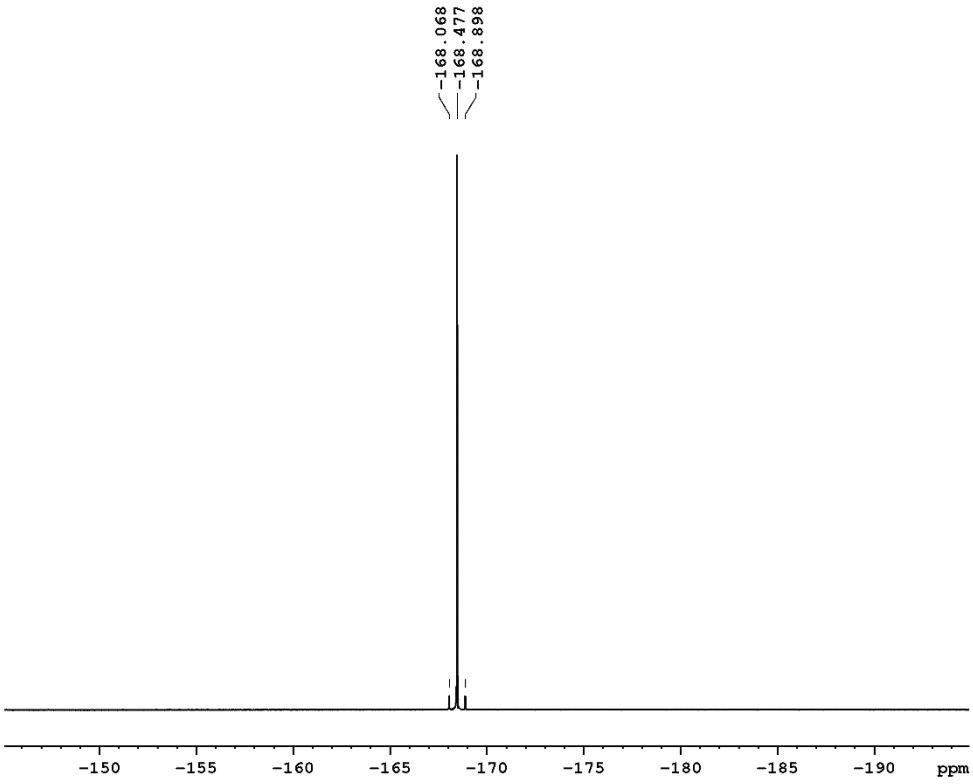

Figure A.5 $^{19}F\{^{1}H\}$ NMR spectrum of Ph_3SiF (d_6-DMSO, 360MHz)

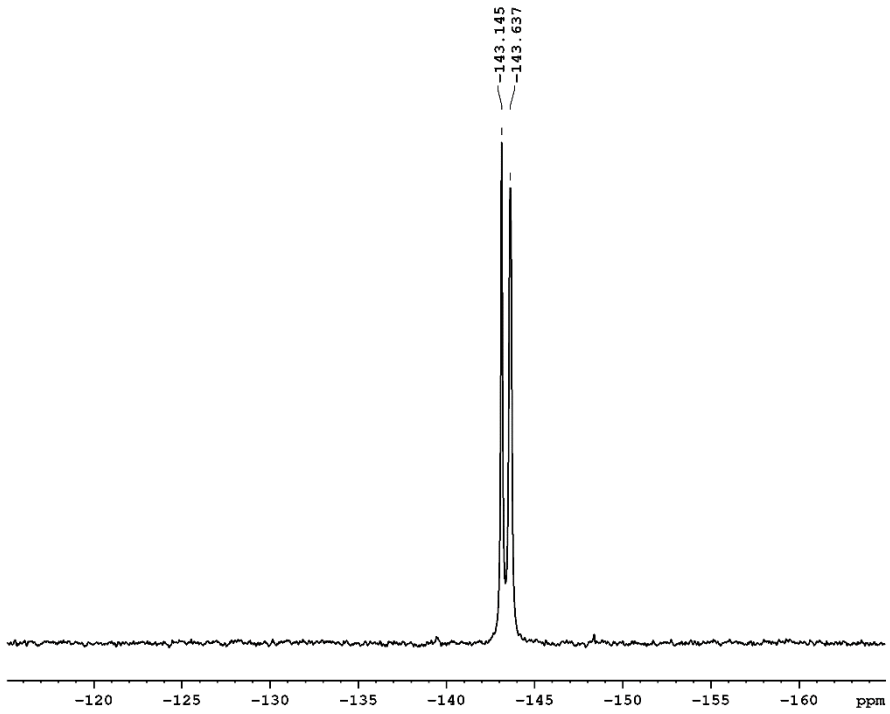

Figure A.6a $^{19}F\{^{1}H\}$ NMR spectrum of $NBu_4F \cdot 3H_2O$ (d_6-DMSO, 360MHz)

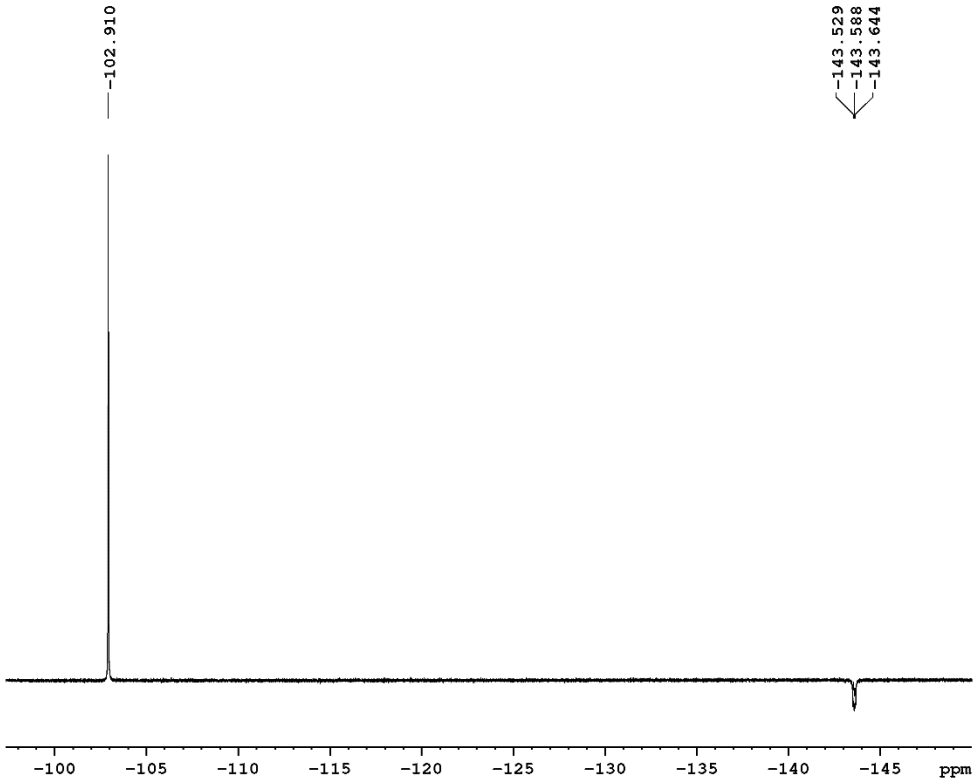

Figure A.6b $^{19}F\{^{1}H\}$ NMR spectrum of $NBu_4F \cdot 3H_2O$ re-acquired after 24 hours (d_6-DMSO, 360MHz)

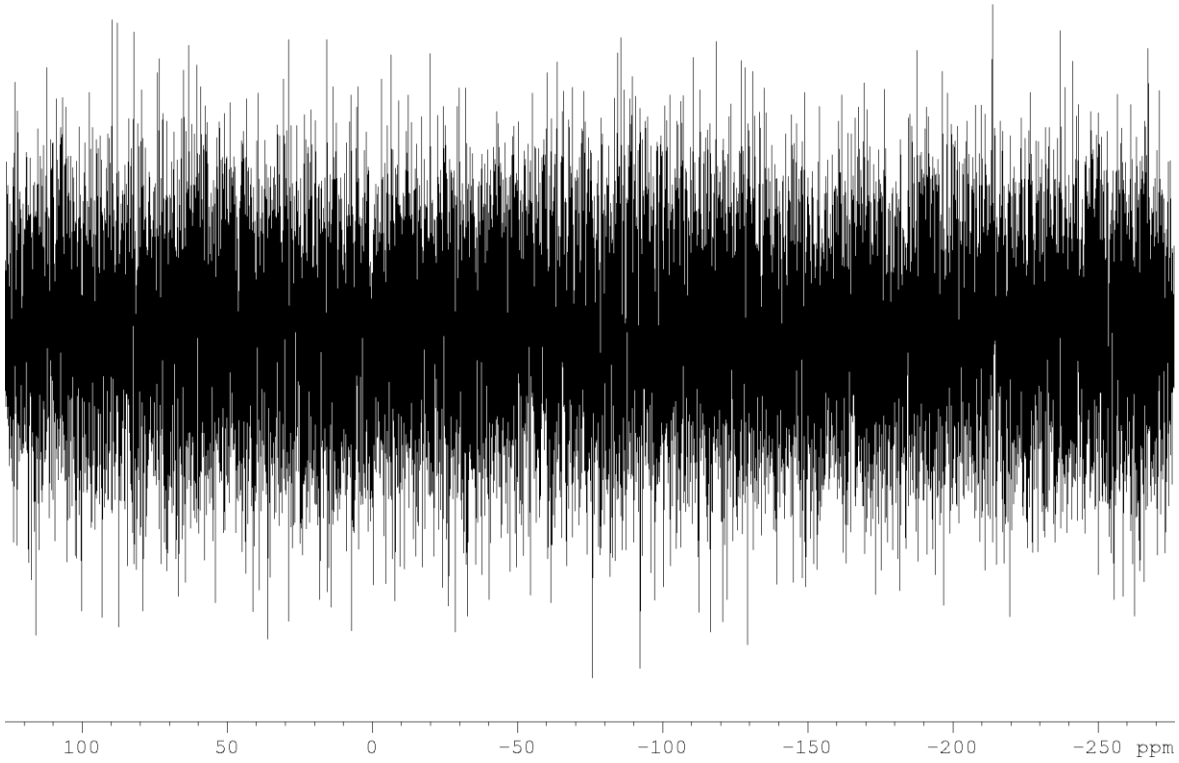

Figure A.7 ^{29}Si DEPT NMR spectrum of Ph_3SiF + 2 equiv. $NBu_4F{\cdot}3H_2O$ in DMF, heated to 110°C for 5 minutes. (d_6-acetone capillary insert, 360MHz)

Appendix B (Alternative Strategies for Molecular Modelling to Improve Comprehension of Molecular Geometry and Enhance Representational Competence)

Table B.1 Summary of descriptive statistics for assessment survey data

Variable	Total Count	Mean	SE Mean	StDev	Variance	95% CI for μ	Skewness	Kurtosis
Pre-Lab (Year 1)	424	2.406	0.048	0.997	0.993	(2.3105, 2.5008)	-0.18	-0.45
Post-Lab (Year 1)	302	2.497	0.062	1.084	1.174	(2.3740, 2.6194)	-0.38	-0.51
Pre-Lab (Year 2)	362	2.359	0.055	1.054	1.112	(2.2501, 2.4681)	-0.22	-0.51
Post-Lab (Year 2)	278	2.284	0.068	1.138	1.294	(2.1498, 2.4185)	-0.12	-0.80
Pre-Lab (Year 3)	522	2.000	0.050	1.149	1.321	(1.9012, 2.0988)	0.08	-0.84
Post-Lab (Year 3)	455	2.389	0.054	1.142	1.304	(2.2838, 2.4942)	-0.16	-0.89

Table B.2 Summary of descriptive statistics for questionnaire data

Variable	N	Mean	SE Mean	StDev	Variance	95% CI for μ	Median	Skewness	Kurtosis
Q1 Y1	303	3.6667	0.0553	0.9617	0.9249	(3.5579, 3.7754)	4	-1.07	1.03
Q1 Y2	225	3.8756	0.0543	0.8143	0.6630	(3.7686, 3.9825)	4	-1.17	2.43
Q1 Y3	486	3.2757	0.0465	1.0245	1.0496	(3.1844, 3.3670)	4	-0.62	-0.30
Q2 Y1	302	3.1258	0.0663	1.1517	1.3263	(2.9954, 3.2562)	3	-0.25	-0.78
Q2 Y2	225	3.4311	0.0806	1.2086	1.4606	(3.2723, 3.5899)	4	-0.59	-0.52
Q2 Y3	453	3.1347	0.0543	1.1548	1.3336	(3.0280, 3.2413)	3	-0.33	-0.72
Q3 Y1	303	3.2508	0.0685	1.1918	1.4203	(3.1161, 3.3856)	3	-0.29	-0.79
Q3 Y2	225	3.3111	0.0797	1.1956	1.4296	(3.1540, 3.4682)	3	-0.32	-0.66
Q3 Y3	475	2.7074	0.0569	1.2396	1.5365	(2.5956, 2.8191)	3	0.20	-0.98

Q = question, Y = Year

Table B.3 Summary of statistical analysis for comparison of sample means for assessment data

Variable	T-Value	P-Value	Difference	95% CI for Difference
Year 1	1.15	0.249	*0.0910 (2.28%)*	*±0.1551 (±3.878%)*
Year 2	-0.85	0.394	*-0.0749 (-1.87%)*	*±0.1727 (±4.316%)*
Year 3	5.30	<0.0001	0.3890 (9.725%)	*±0.1442* (±3.604%)

μ_1: mean of Post-Lab Scores
μ_2: mean of Pre-Lab Scores
Difference: $\mu_1 - \mu_2$
Null hypothesis H_0: $\mu_1 - \mu_2 = 0$
Alternative hypothesis H_1: $\mu_1 - \mu_2 \neq 0$
Null hypothesis is rejected for p-values < 0.05

Table B.4 Summary of statistical analysis for comparison of sample means and medians for questionnaire data

	Question 1		Question 2		Question 3	
	Δx[a]	MWU[b]	Δx[a]	MWU[b]	Δx[a]	MWU[b]
$\mu_{Y2} - \mu_{Y1}$	0.21± 0.15**	*	-0.31 ± 0.21**	***	NS	NS
$\mu_{Y3} - \mu_{Y1}$	-0.39 ± 0.14***	***	NS	NS	-0.54± 0.17 ***	***
$\mu_{Y3} - \mu_{Y2}$	-0.60±0.14 ***	***	-0.30± 0.19 **	***	-0.60± 0.19 ***	***

[a] Δx = difference between two sample means ($\mu_a - \mu_b$), determined from two-sample t-test (α=0.05)
[b] Mann-Whitney U Test (MWU) (α=0.05), adjusted for ties
$* \; p \leq 0.05$; $** \; p \leq 0.01$; $*** \; p \leq 0.001$; $NS \; (not \; significant) \; p > 0.05$

University of Victoria

Letter of Information for Implied Consent

Improving Student Understanding of Molecular Geometry using Handheld 3D Printing

You are invited to participate in a study that is being conducted by Dr. Scott McIndoe and Corrina Ewan.

Dr. McIndoe is a faculty member in the department of chemistry at the University of Victoria and you may contact him if you have further questions by e-mail at [redacted].

Purpose and Objectives
The purpose of this research project is to examine the effect that adding a third dimension to a student's ability to draw molecules has on their understanding of molecular structure.

Importance of this Research
Research of this type is important because grasping the relationship between a two-dimensional representation and the corresponding three-dimensional object is a critical concept in chemistry, and we want to make sure that you, as students, are being provided with the most effective learning experience.

Participants Selection
You are being asked to participate in this study because you are a Chemistry 101 student

What is involved
If you consent to voluntarily participate in this research, your participation will include completing two brief 5-minute surveys, before and after you have completed the laboratory exercise.

Inconvenience
Participation in this study may cause some inconvenience to you, including losing approximately 10 minutes of dedicated lab time.

Risks
There are some potential risks to you by participating in this research and they include the potential of feeling stressed or discomfort from completing the surveys, as some of the questions resemble a quiz in that they assess knowledge of the course material. To prevent or to deal with these risks we would like to remind you that the surveys are both anonymous and not for marks and therefore there is no need to feel stress/discomfort when completing them. If you experience stress or discomfort while completing the surveys, you may withdraw from the study at any point by not completing the survey.

Benefits
The potential benefits of your participation in this research include: an improved lab experience, improved spatial abilities and contributing to the assessment and possible improvement of model building exercises in academic settings.

Voluntary Participation
Your participation in this research must be completely voluntary. If you do decide to participate, you may withdraw at any time without any consequences or any explanation. If you do withdraw from the study your data will not be removed from the study, as it is logistically impossible due to the anonymous nature of the study.

Researcher's Relationship with Participants
The researcher may have a relationship to potential participants as professor/student. To help prevent this relationship from influencing your decision to participate, the following steps to prevent coercion have been taken: Dr. McIndoe will not be present during the time the participant will be completing the surveys. Participants are reminded that (1) participation in the research is voluntary, (2) no one will know who has participated or not because the surveys are anonymous, and the instructor will not be present during the completing of the surveys, and (3) grades and class standing will not be affected whether students choose to participate or not.

Anonymity & Confidentiality
Your anonymity, confidentiality and the confidentiality of the data will be completely protected throughout the data gathering phase as well as the dissemination of the results. This will be achieved through the anonymous nature of the survey, as well as by having the researcher leave the room while you complete the surveys.

Dissemination of Results
It is anticipated that the results of this study will be shared with others in the following ways: thesis/dissertation, published article(s) and presentations at scholarly meetings.

Disposal of Data
Data from this study will be disposed of by shredding surveys.

Contacts
Individuals that may be contacted regarding this study include: Dr. Scott McIndoe and Corrina Ewan.

In addition, you may verify the ethical approval of this study, or raise any concerns you might have, by contacting the Human Research Ethics Office at the University of Victoria.

By completing and submitting the questionnaire, **YOUR FREE AND INFORMED CONSENT IS IMPLIED** and indicates that you understand the above conditions of participation in this study and that you have had the opportunity to have your questions answered by the researchers.

Please retain a copy of this letter for your reference.